

Table of contents

Materials, measurement and instrumentation (p S2)
Synthesis and characterization of precursors and comonomers (p S3-S4)
Synthesis and characterization of model compounds (p S5)
NMR spectra for compounds **1**, **2**, **5**, **7**, **8**, **MC-1** and **MC-2** (p S6-S12)
Complementary information about X-ray single crystal analysis (p S13-S15)
Spatial arrangement of carbazole derivative **2** (p S16)
Complementary information about electrochemical properties (p S17)
Complementary information about thermal properties of comonomers (p S18-S19)
Complementary information about UV/Vis absorption properties (p S20)
Complementary information about visualizations of molecular orbitals (p S21)
Synthesis of PI films (p S22)
FTIR spectroscopy (p S23-S24)
Photophysical properties of model compounds (p S25)
Photographs of PI films (p S26)
CIE chromaticity diagrams of PI films (p S27)
Complementary information about thermal properties of PI films (p S28)
References (p S29)

Materials, measurement and instrumentation

All commercial chemicals, reagents and solvents were purchased from Sigma Aldrich (Merck), Acros, TCI, and Penta and were used without further purification.

Column chromatography was carried out with silica gel 60 (particle size 0.040–0.063 mm, 230–400 mesh; Merck) and commercially available solvents.

Thin-layer chromatography (TLC) was conducted on aluminium sheets coated with silica gel 60 F254, obtained from Merck, with visualization by a UV lamp (254 or 365 nm).

^1H and ^{13}C NMR spectra were recorded at 500 and 125 MHz with a Bruker Ascend TM 500 at 25 °C. Chemical shifts are reported in ppm relative to the signal of Me_4Si . The residual solvent signal in the ^1H and ^{13}C NMR spectra was used as an internal reference (CDCl_3 $\delta = 7.25$ and 77.24 ppm). Apparent resonance multiplicities are described as s (singlet), br. s (broad singlet) and m (multiplet).

High-resolution MALDI MS spectra were measured with a MALDI mass spectrometer LTQ Orbitrap XL (Thermo Fisher Scientific, Bremen, Germany) equipped with nitrogen UV laser (337 nm, 60 Hz). The LTQ Orbitrap instrument was operated in positive-ion mode over a normal mass range (m/z 50–2000) with resolution 100 000 at $m/z = 400$. The survey crystal positioning system (survey CPS) was set for the random choice of shot position by automatic crystal recognition. *trans*-2-[3-(4-*tert*Butylphenyl)-2-methyl-2-propenylidene]malononitrile (DCTB) was used as a matrix. Mass spectra were averaged over the whole MS record for all measured samples.

Transmittance, absorption and fluorescence spectra were measured on a Duetta™ HORIBA spectrophotometer in DCM and THF solutes at room temperature, for comonomers and in solid state for PI films.

Voltammetric measurements were performed by using an integrated potentiostat system ER466 (eDAQ) operated with EChem Electrochemistry software.

Thermal properties of **1** and **2** were measured by differential scanning calorimetry DSC on a Mettler-Toledo STARE System DSC 2/700 equipped with an FRS 6 ceramic sensor and HUBER TC100-MT RC 23 cooling system in open aluminum crucibles sealed with a pierced lid under an N_2 atmosphere. DSC curves were obtained at a scanning rate of 3 °C min^{-1} .

DFT calculations were performed using Gaussian 16W.

The X-ray data for colorless crystal of **1** were obtained at 150 K using Oxford Cryostream low-temperature device with a Bruker D8-Venture diffractometer equipped with Mo ($\text{Mo}/\text{K}\alpha$ radiation; $\lambda = 0.71073$ Å) microfocus X-ray ($1\mu\text{S}$) source, Photon CMOS detector and Oxford Cryosystems cooling device was used for data collection. Obtained data were treated by XT-version 2014/5 and SHELXL-2017/1 software implemented in APEX3 v2016.9-0 (Bruker AXS) system.

Glass transition temperature of polyimides was measured using DCS 250 (TA Instruments, New Castle, DE, USA) under nitrogen gas flow with a heating rate of 20 °C/min with range 25–300 °C in closed aluminum sample pan.

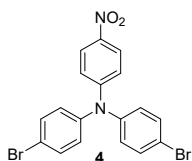
Thermal stability of **1**, **2** and polyimides was carried out with a TGA Q500 (TA Instruments, New Castle, DE, USA) under nitrogen gas flow with a heating rate of 3 or 10 °C/min with the range 25–600 °C in open platinum sample pan.

Thickness of the PI films was measured using KMITEX Digital Micrometer IP 65, DIN 863, ABS, range 0 – 25 mm, resolution 0.001 mm.

IR spectra were recorded as neat by using HATR adapter with a Perkin–Elmer FTIR Spectrum BX spectrometer.

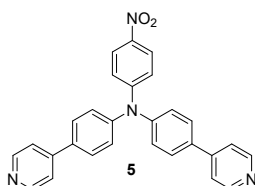
Synthesis of amines

2.3.1. 4-Bromo-*N*-(4-bromophenyl)-*N*-(4-nitrophenyl)aniline (4)



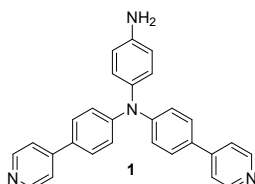
In a round-bottomed flask equipped with a magnetic stirrer, 4-bromo-*N*-(4-bromophenyl)aniline **3** (500 mg, 1.53 mmol), 1-fluoro-4-nitrobenzene (243 μ L, 2.29 mmol), K_2CO_3 (317 mg, 2.29 mmol) and DMSO (10 mL) were mixed and stirred for 12 h at 145 $^{\circ}C$. The mixture was then cooled to room temperature. Precipitate was collected by vacuum filtration, washed with water and cold ethanol, and dried under vacuum to give compound **4** as a yellow solid (561 mg, 82%). The spectral characterization corresponds to that reported in the literature.[1]

4-Nitro-*N,N*-bis(4-(pyridin-4-yl)phenyl)aniline (5)



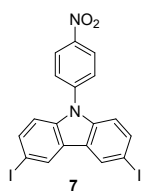
In a vacuo-dried Schlenk tube under an inert atmosphere of argon equipped with a magnetic stirrer, precursor **4** (561 mg, 1.25 mmol), pyridin-4-ylboronic acid (339 mg, 2.21 mg), Na_2CO_3 (265 mg, 2.50 mmol) and dioxane/water 4:1 (25 mL) were mixed. Argon was bubbled through the mixture for 5 min and $PdCl_2(PPh_3)_2$ (35 mg, 0.05 mmol) was added and reaction mixture was stirred for 12 h at 90 $^{\circ}C$. The mixture was then cooled down to room temperature, diluted with saturated solution of $NaHCO_3$ (50 mL) and extracted with DCM (2 \times 50 mL). The combined organic extracts were then washed with brine (50 mL) and dried with Na_2SO_4 . Finally, the solvents were evaporated under vacuum and the crude product was purified by column chromatography (SiO_2 , EtOAc/MeOH 10:1) R_f : 0.3. Nitro derivative **5** was isolated as a yellow solid (529 mg, 95%). Mp: 194 $^{\circ}C$. 1H NMR (500 MHz, $CDCl_3$): δ (ppm) 7.10–7.12 (m, 2H), 7.29–7.31 (m, 4H), 7.49–7.50 (m, 4H), 7.64–7.66 (m, 4H), 8.10–8.12 (m, 2H), 8.66–8.67 (m, 4H). ^{13}C NMR (125 MHz, $CDCl_3$): δ (ppm) 120.4, 121.5, 125.8, 126.6, 128.8, 135.3, 141.6, 146.7, 147.3, 150.6, 152.8. HRMS (MALDI) m/z calc. for $C_{28}H_{20}N_4O_2$: 445.1659 [M^+], found 445.1642.

*N*¹,*N*¹-Bis(4-(pyridin-4-yl)phenyl)benzene-1,4-diamine (1)



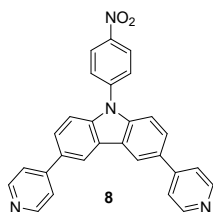
Following previously described protocol,[2] in a round-bottomed flask equipped with a magnetic stirrer and dry ethanol (10 mL), precursor **5** (529 mg, 1.19 mmol) and Pd/C (10%, 17 mg) were mixed and stirred for 1 h under reflux. After 1-hour period hydrazine hydrate (80%, 397 μ L) was added dropwise. Reaction mixture was refluxed for 12 h, then cooled down to room temperature, diluted with saturated solution of $NaHCO_3$ (50 mL) and extracted with DCM (2 \times 50 mL). The combined organic extracts were then washed with brine (50 mL) and dried with Na_2SO_4 . Finally, the solvents were evaporated under vacuum and the product was precipitated from chloroform solution with hexane. Amino derivative **1** was isolated as a light brown solid (385 mg, 78%). Mp: 122 $^{\circ}C$. 1H NMR (500 MHz, $CDCl_3$): δ (ppm) 3.71 (br. s, 2H), 6.69–6.70 (m, 2H), 7.00–7.02 (m, 2H), 7.15–7.17 (m, 4H), 7.46–7.47 (m, 4H), 7.51–7.53 (m, 4H), 8.60–8.61 (m, 4H). ^{13}C NMR (125 MHz, $CDCl_3$): δ (ppm) 116.5, 121.1, 122.8, 127.9, 128.6, 131.1, 137.7, 144.4, 147.9, 148.8, 150.4. HRMS (MALDI) m/z calc. for $C_{28}H_{22}N_4$: 414.1839 [M^+], found 414.1829.

3,6-Diiodo-9-(4-nitrophenyl)-9H-carbazole (7)



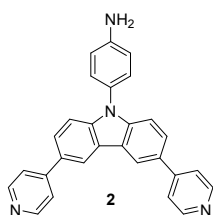
The synthetic procedure was similar to that used for the synthesis of **4**. Starting from 3,6-diiodo-9H-carbazole **6** (641 mg, 1.53 mmol), compound **7** was obtained as a yellow solid (727 mg, 88%). Mp: 276 °C. ¹H NMR (500 MHz, CDCl₃): δ (ppm) 7.21–7.23 (m, 2H), 7.70–7.73 (m, 4H), 8.39–8.39 (m, 2H), 8.48–8.50 (m, 2H). ¹³C NMR (125 MHz, CDCl₃): δ (ppm) 84.4, 111.9, 125.3, 126.0, 127.1, 130.0, 135.7, 139.4, 142.9, 146.6. HRMS (MALDI) *m/z* calc. for C₁₈H₁₀I₂N₂O₂: 539.8830 [M⁺], found 539.8826.

9-(4-Nitrophenyl)-3,6-di(pyridin-4-yl)-9H-carbazole (8)



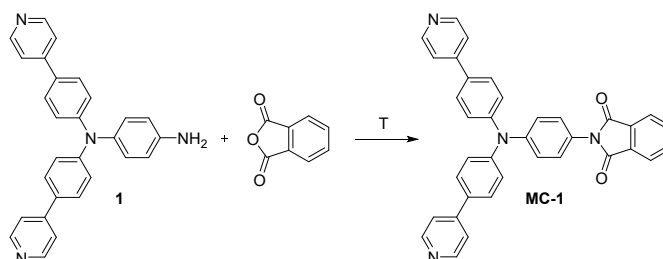
The synthetic procedure was similar to that used for synthesis of **5**. Starting from precursor **7** (1.35 g, 2.5 mmol) and pyridin-4-ylboronic acid (678 mg, 4.42 mg), Na₂CO₃ (530 mg, 5.0 mmol) and dioxane/water 4:1 (25 mL), compound **8** was obtained as a yellow solid (586 mg, 53%) after column chromatography (SiO₂, EtOAc/MeOH 10:1) *R_f*: 0.25. Mp: 338 °C. ¹H NMR (500 MHz, CDCl₃): δ (ppm) 7.59–7.61 (m, 2H), 7.65–7.66 (m, 4H), 7.78–7.80 (m, 2H), 7.84–7.86 (m, 2H), 8.49 (s, 2H), 8.55–8.56 (m, 2H), 8.70–8.71 (m, 4H). ¹³C NMR (125 MHz, CDCl₃): δ (ppm) 110.8, 119.6, 121.9, 124.9, 126.0, 126.3, 127.1, 132.1, 141.1, 143.2, 146.6, 148.6, 150.6. HRMS (MALDI) *m/z* calc. for C₂₈H₁₈N₄O₂: 442.1424 [M⁺], found 442.1436.

4-(3,6-Di(pyridin-4-yl)-9H-carbazol-9-yl)aniline (2)



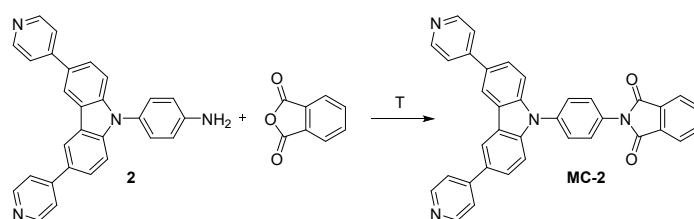
The synthetic procedure was similar to that used for the synthesis of **1**. Starting from 9-(4-nitrophenyl)-3,6-di(pyridin-4-yl)-9H-carbazole **8** (527 mg, 1.19 mmol), compound **2** was obtained as a light beige solid (231 mg, 47%) after precipitation. Mp: 349 °C. ¹H NMR (500 MHz, CDCl₃): δ (ppm) 3.94 (s, 2H), 6.90–6.91 (m, 2H), 7.31–7.33 (m, 2H), 7.42–7.44 (m, 2H), 7.65–7.66 (m, 4H), 7.72–7.74 (m, 2H), 8.48 (s, 2H), 8.67–8.68 (m, 4H). ¹³C NMR (125 MHz, CDCl₃): δ (ppm) 111.0, 116.2, 119.2, 121.9, 123.8, 125.6, 127.5, 128.6, 130.3, 142.8, 146.8, 149.2, 150.5. HRMS (MALDI) *m/z* calc. for C₂₈H₂₀N₄: 412.1683 [M⁺], found 412.1681.

Synthesis and characterization of model compounds:



Scheme S1. Synthesis of model compound **MC-1**.

In a round-bottomed flask compound **1** (50 mg, 0.121 mmol) and phthalic anhydride (21 mg, 0.145 mmol) were mixed and heated neat to 150 °C for period of 5 min and 170 °C for subsequent 5 min. The mixture was then cooled to room temperature, dissolved in DCM (50 ml) and extracted with saturated solution of NaHCO₃ (50 mL), water fraction was then extracted one more time with DCM (50 mL). The combined organic extracts were then washed with brine (50 mL) and dried with Na₂SO₄. Finally, the solvents were evaporated under vacuum and the crude product was purified by column chromatography (SiO₂, EtOAc/MeOH 5:1) *R_f*: 0.5. Model compound **MC-1** was isolated as the yellow solid (63 mg, 95 %). Mp: 301 °C. ¹H NMR (500 MHz, CDCl₃): δ (ppm) 7.27–7.28 (m, 6H), 7.37–7.39 (m, 2H), 7.50–7.51 (m, 4H), 7.58–7.61 (m, 4H), 7.79–7.81 (m, 2H), 7.95–7.97 (m, 2H), 8.63–8.64 (m, 4H). ¹³C NMR (125 MHz, CDCl₃): δ (ppm) 121.32, 124.03, 124.84, 125.09, 127.19, 127.87, 128.30, 131.93, 132.85, 134.73, 146.62, 147.88, 148.22, 150.24, 167.64. HRMS (MALDI) *m/z* calc. for C₃₆H₂₄N₄O₂:544.1894 [M⁺], found 544.1880.



Scheme S2. Synthesis of model compound **MC-2**.

In a round-bottomed flask compound **2** (50 mg, 0.121 mmol) and phthalic anhydride (22 mg, 0.146 mmol) were mixed and heated neat to 150 °C for period of 5 min and 170 °C for subsequent 5 min. The mixture was then cooled to room temperature, dissolved in DCM (50 ml) and extracted with saturated solution of NaHCO₃ (50 mL), water fraction was then extracted one more time with DCM (50 mL). The combined organic extracts were then washed with brine (50 mL) and dried with Na₂SO₄. Finally, the solvents were evaporated under vacuum and the crude product was purified by column chromatography (SiO₂, EtOAc/MeOH 5:1) *R_f*: 0.4. Model compound **MC-2** was isolated as the yellow solid (53 mg, 80 %). Mp: 304 °C. ¹H NMR (500 MHz, CDCl₃): δ (ppm) 7.60–7.62 (m, 2H), 7.67–7.68 (m, 4H), 7.75–7.80 (m, 6H), 7.85–7.87 (m, 2H), 8.02–8.04 (m, 2H), 8.49–8.50 (m, 2H), 8.69–8.70 (m, 4H). ¹³C NMR (125 MHz, CDCl₃): δ (ppm) 111.09, 119.38, 121.97, 124.27, 124.34, 125.99, 127.75, 128.31, 131.02, 131.50, 131.84, 135.00, 136.63, 141.98, 149.14, 150.32, 167.39. HRMS (MALDI) *m/z* calc. for C₃₆H₂₂N₄O₂:542.1737 [M⁺], found 542.1732.

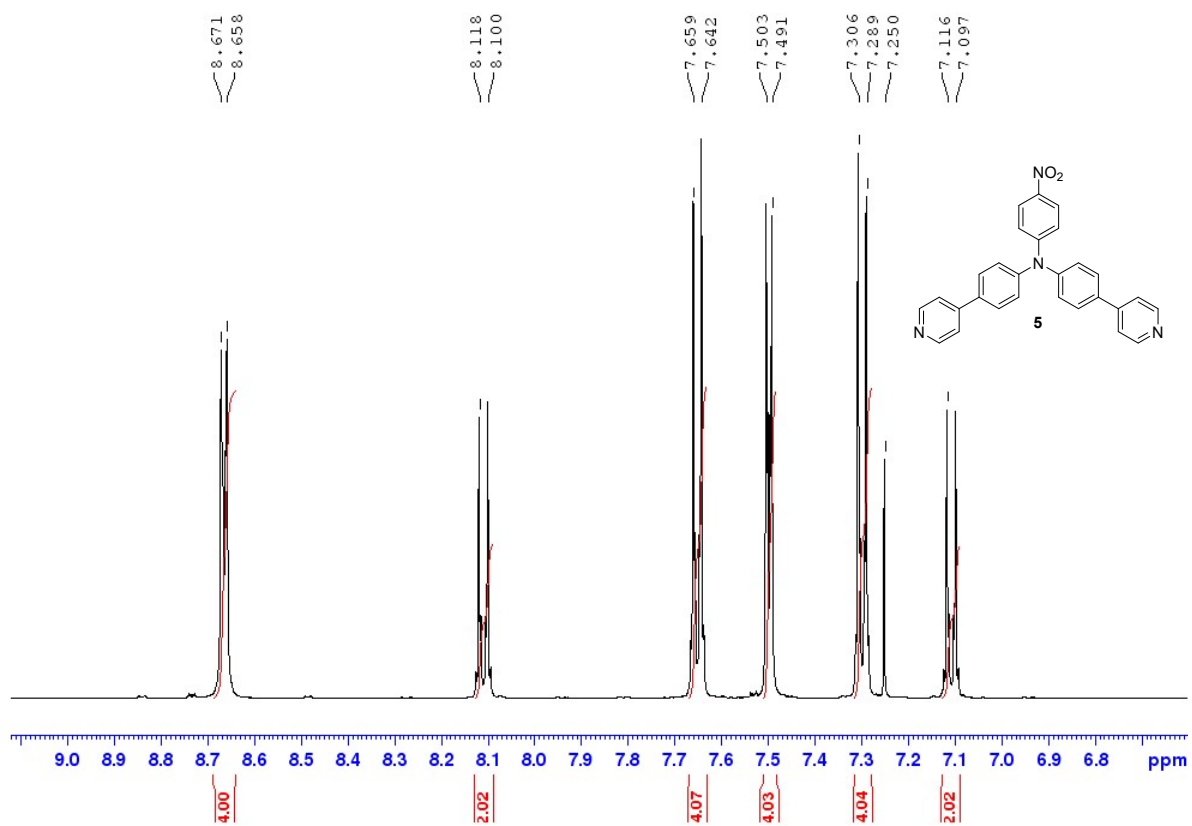


Fig. S1. ^1H NMR (500 MHz, CDCl_3) compound 5.

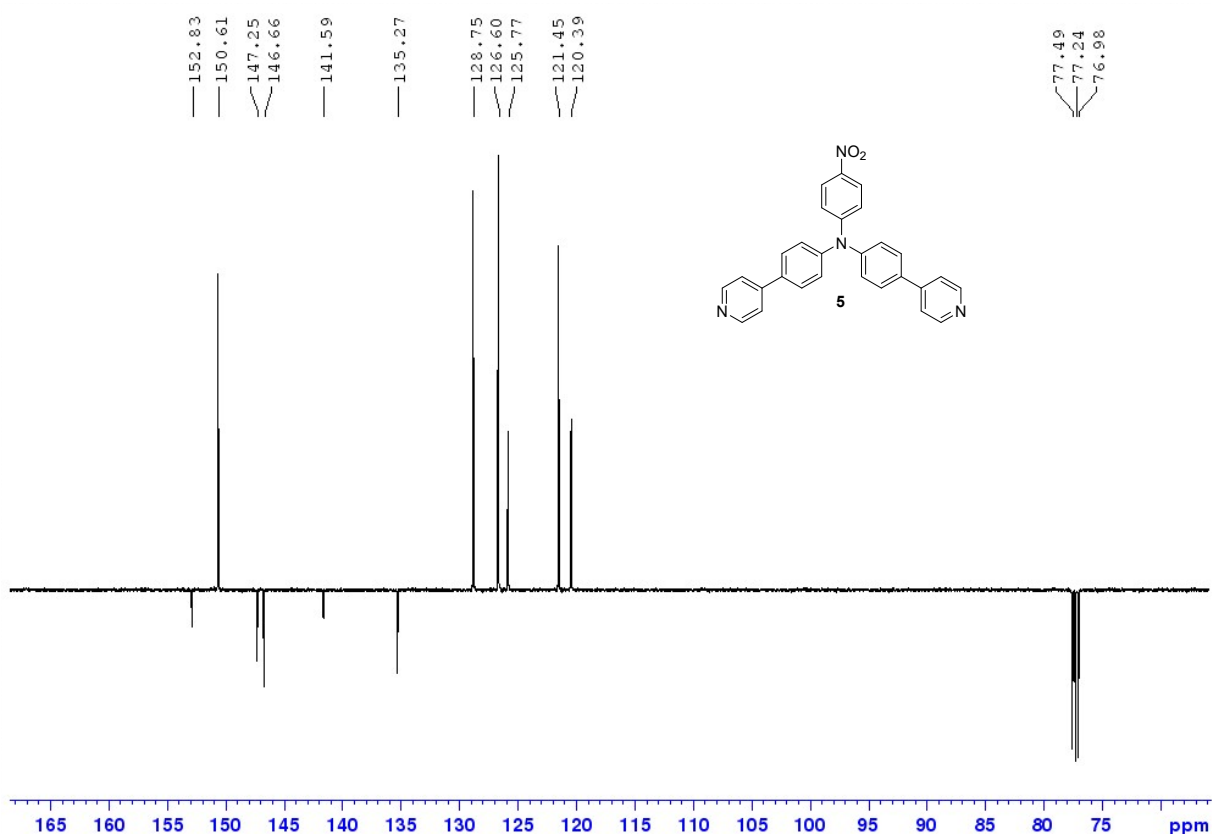


Fig. S2. ^{13}C APT NMR (125 MHz, CDCl_3) compound 5.

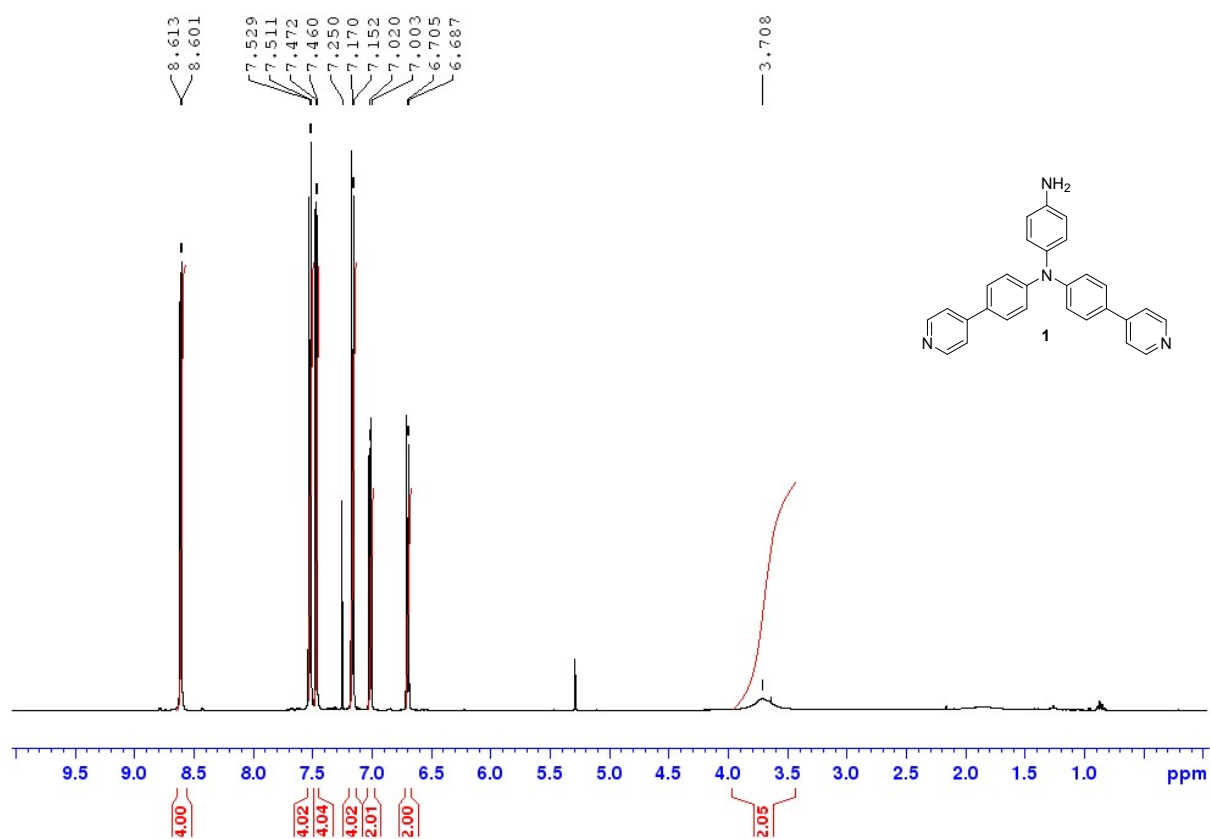


Fig. S3. ¹H NMR (500 MHz, CDCl₃) compound 1.

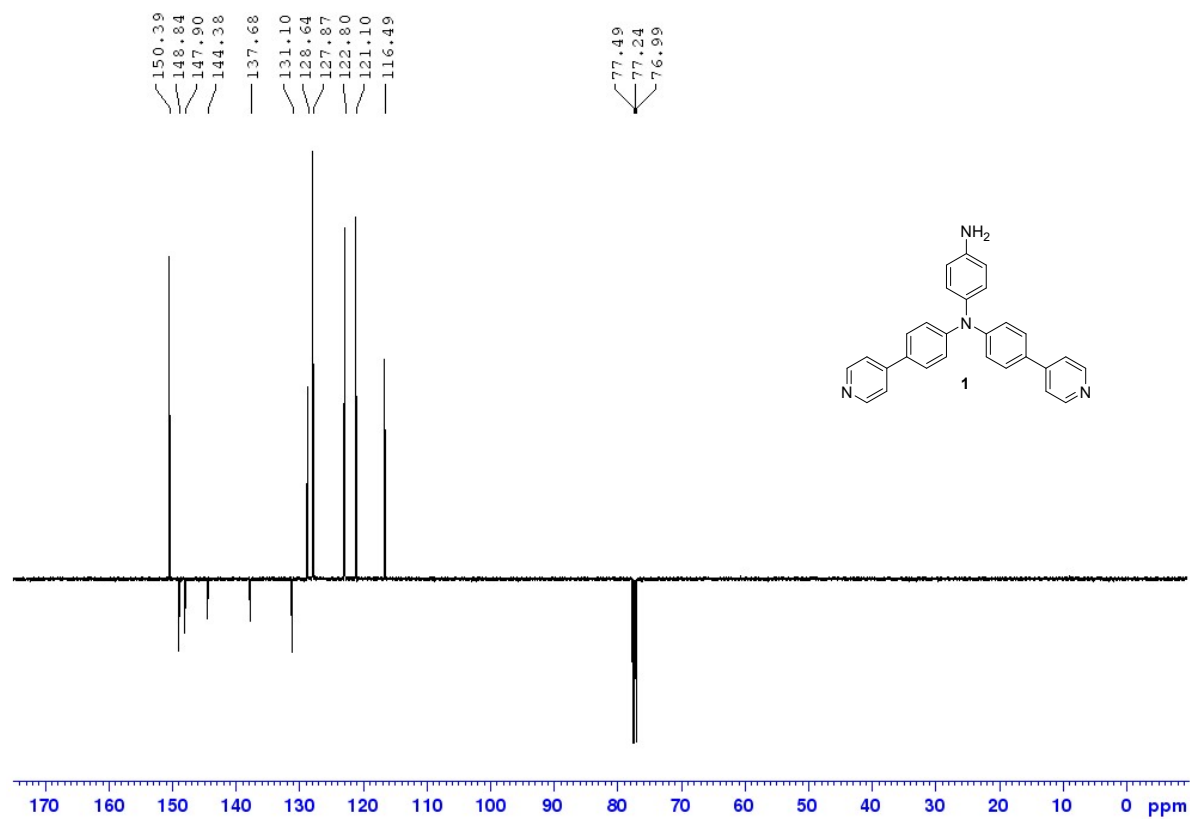


Fig. S4. ¹³C APT NMR (125 MHz, CDCl₃) compound 1.

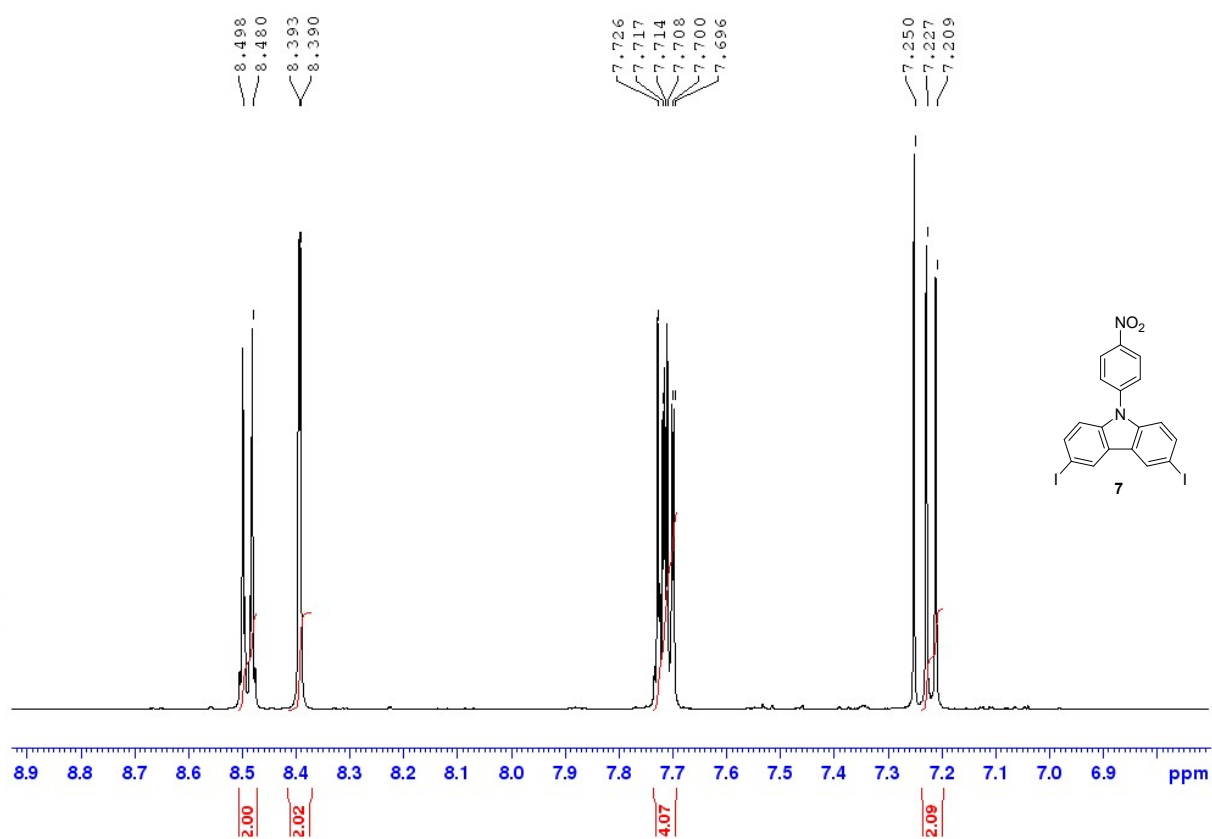


Fig. S5. ^1H NMR (500 MHz, CDCl_3) compound 7.

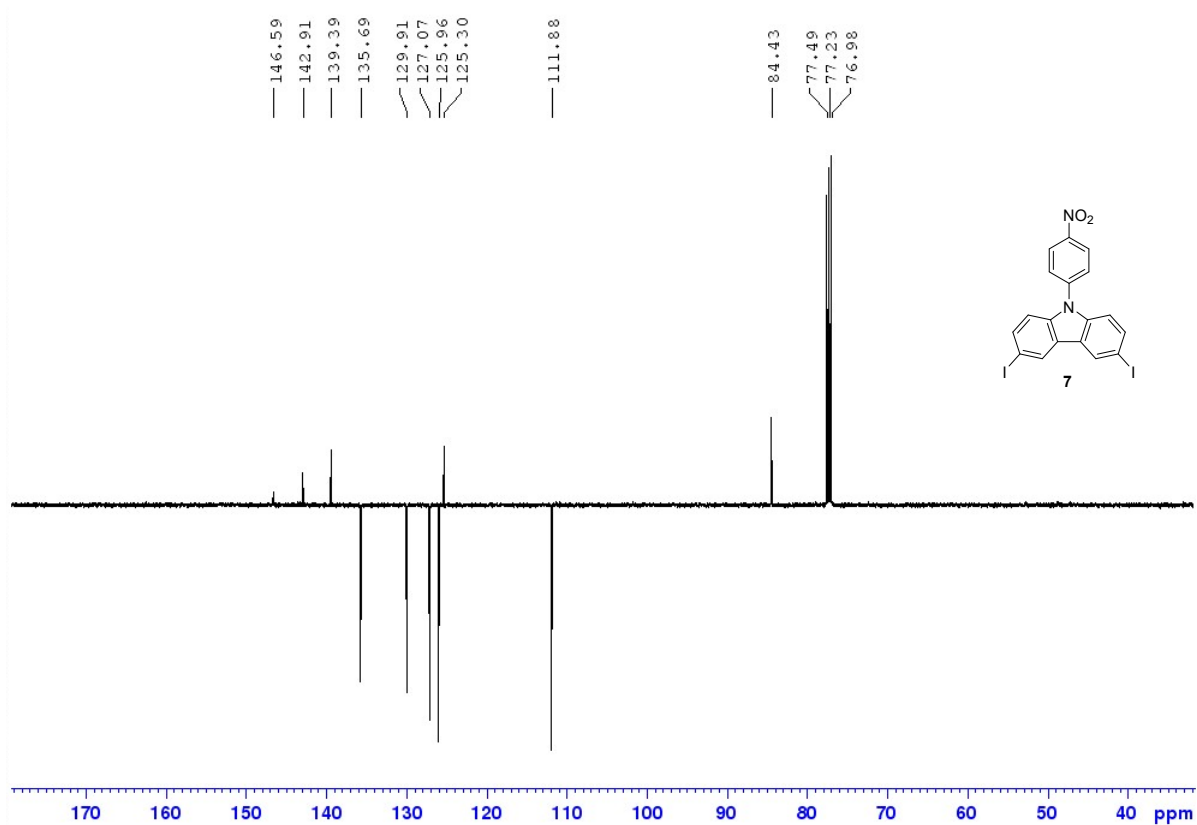


Fig. S6. ^{13}C APT NMR (125 MHz, CDCl_3) compound 7.

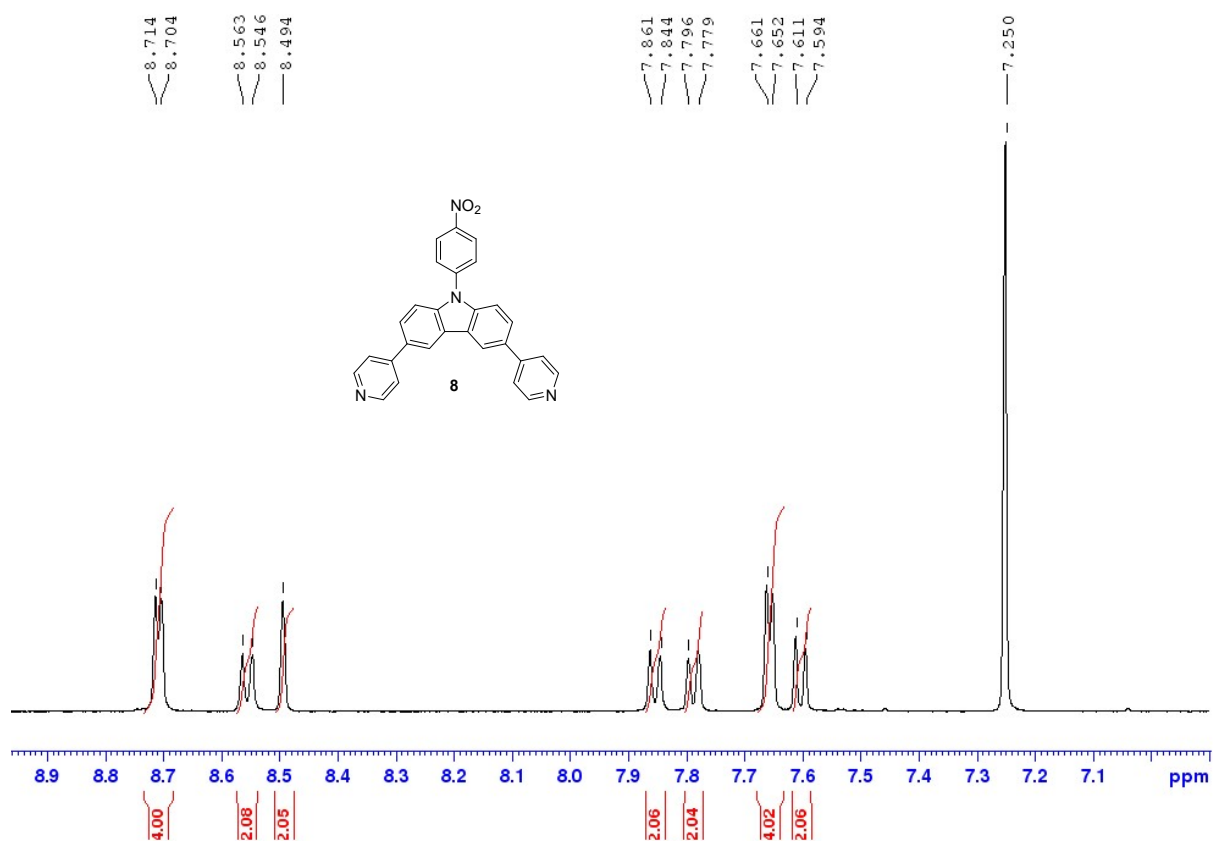


Fig. S7. ^1H NMR (500 MHz, CDCl_3) compound 8.

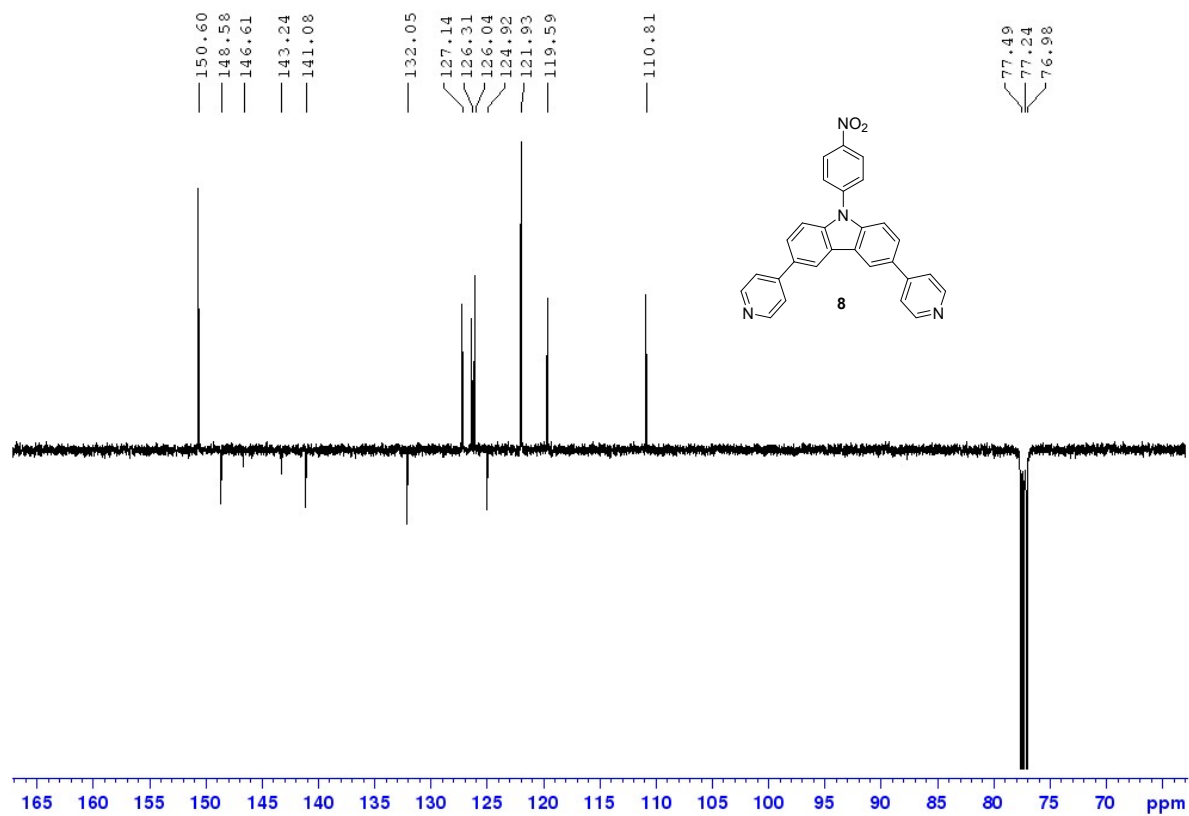


Fig. S8. ^{13}C APT NMR (125 MHz, CDCl_3) compound 8.

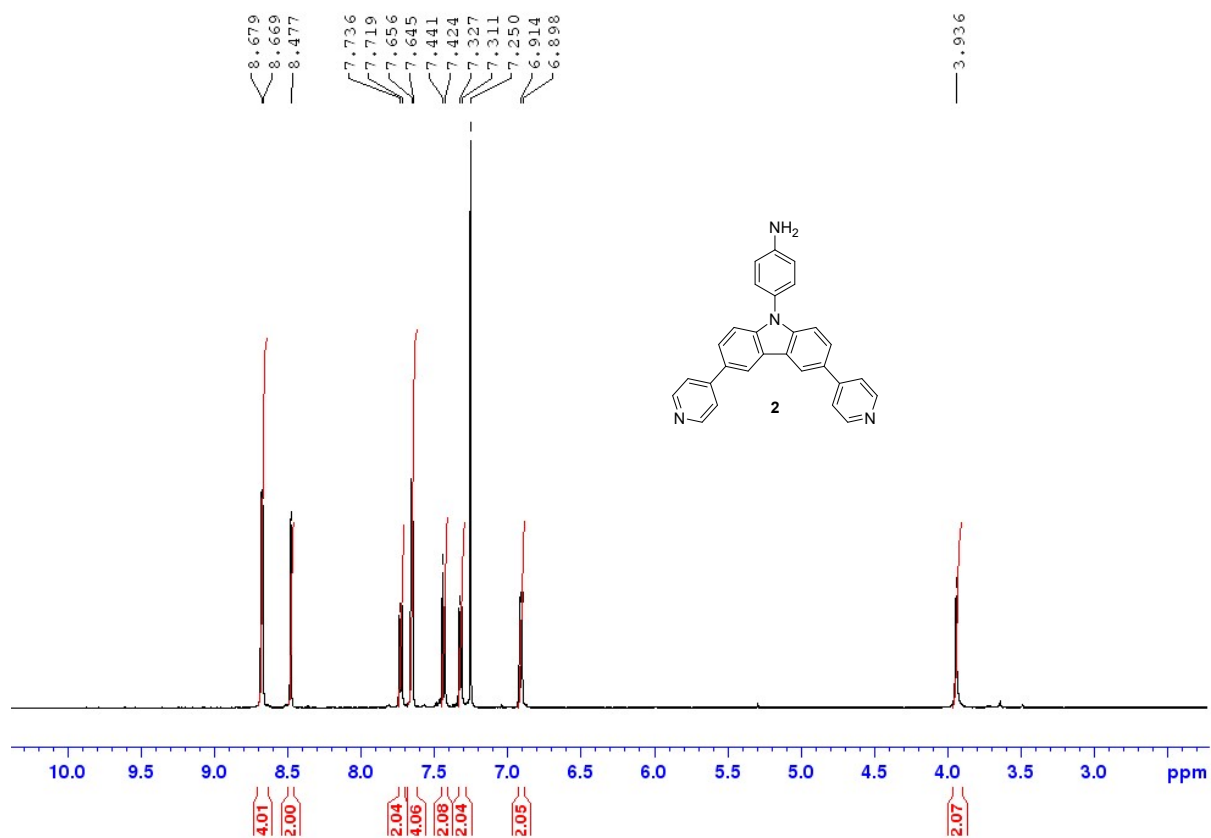


Fig. S9. ^1H NMR (500 MHz, CDCl_3) compound 2.

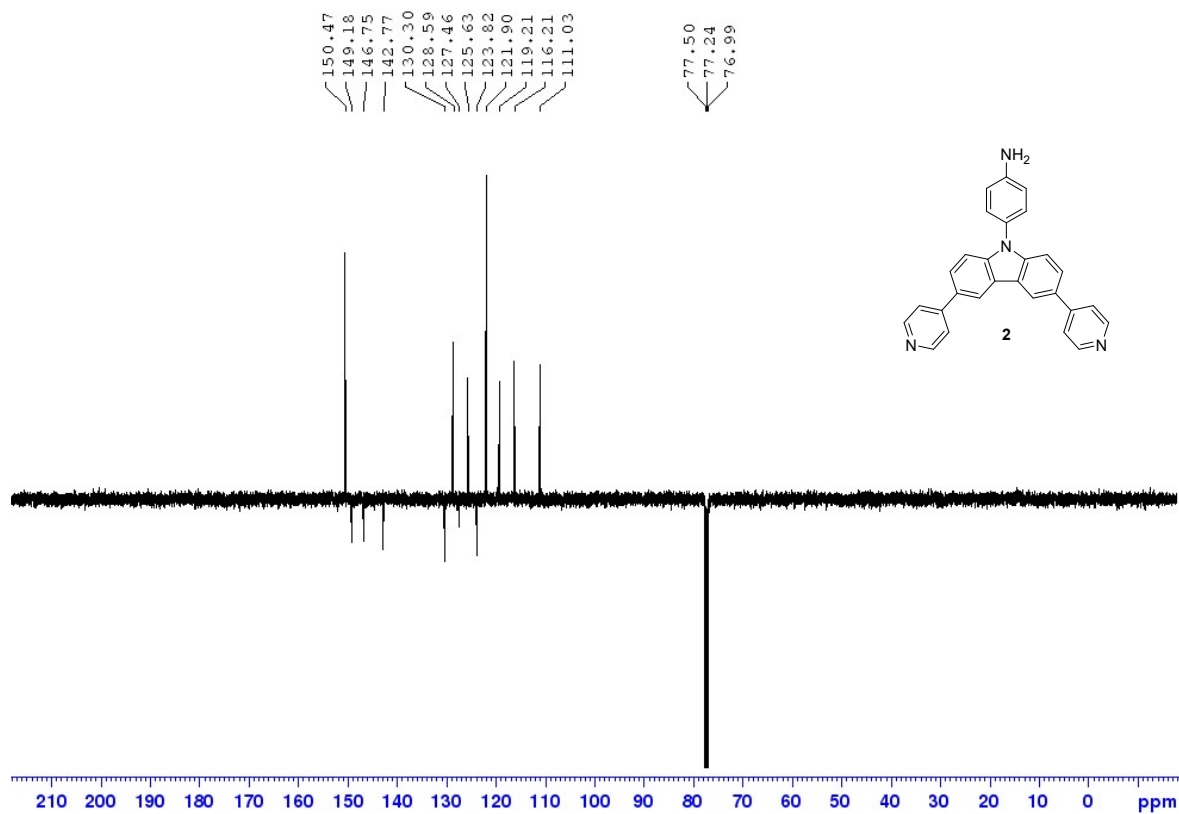


Fig. S10. ^{13}C APT NMR (125 MHz, CDCl_3) compound 2.

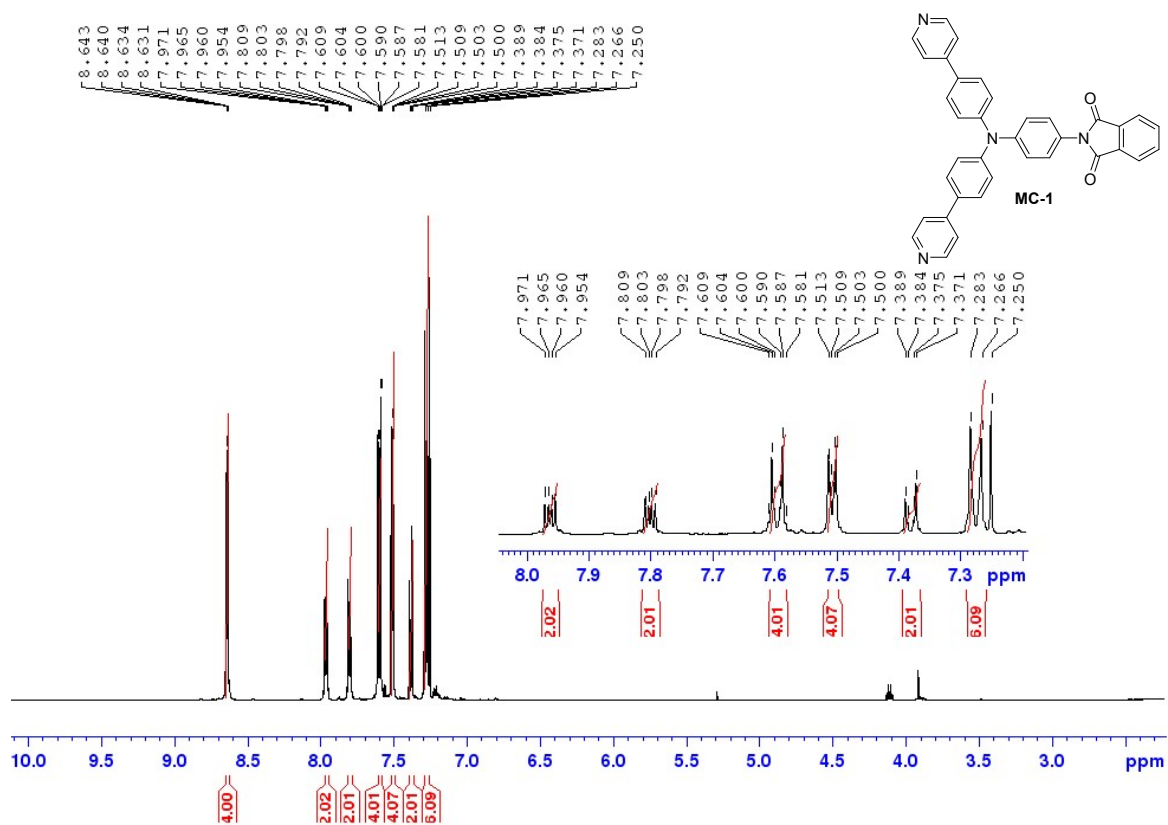


Fig. S11. ¹H NMR (500 MHz, CDCl₃) compound MC-1.

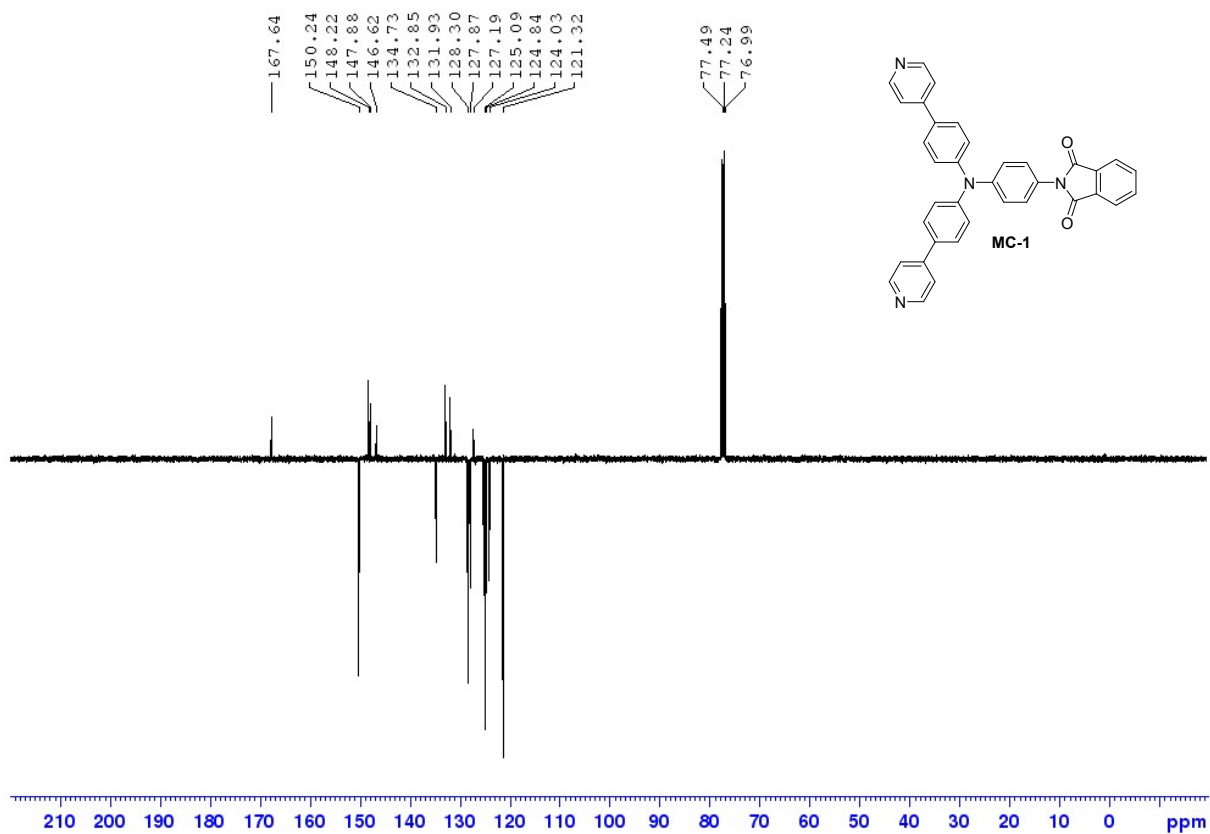


Fig. S12. ¹³C APT NMR (125 MHz, CDCl₃) compound MC-1.

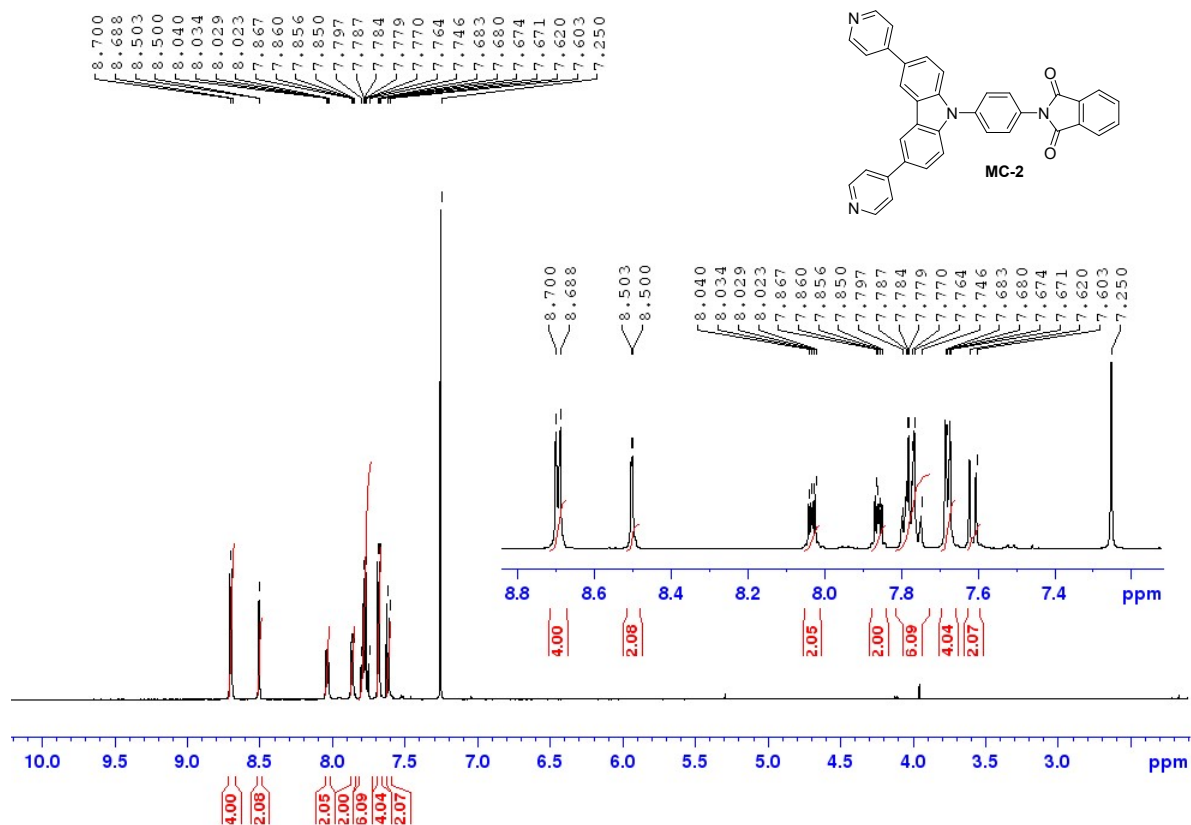


Fig. S13. ¹H NMR (500 MHz, CDCl₃) compound MC-2.

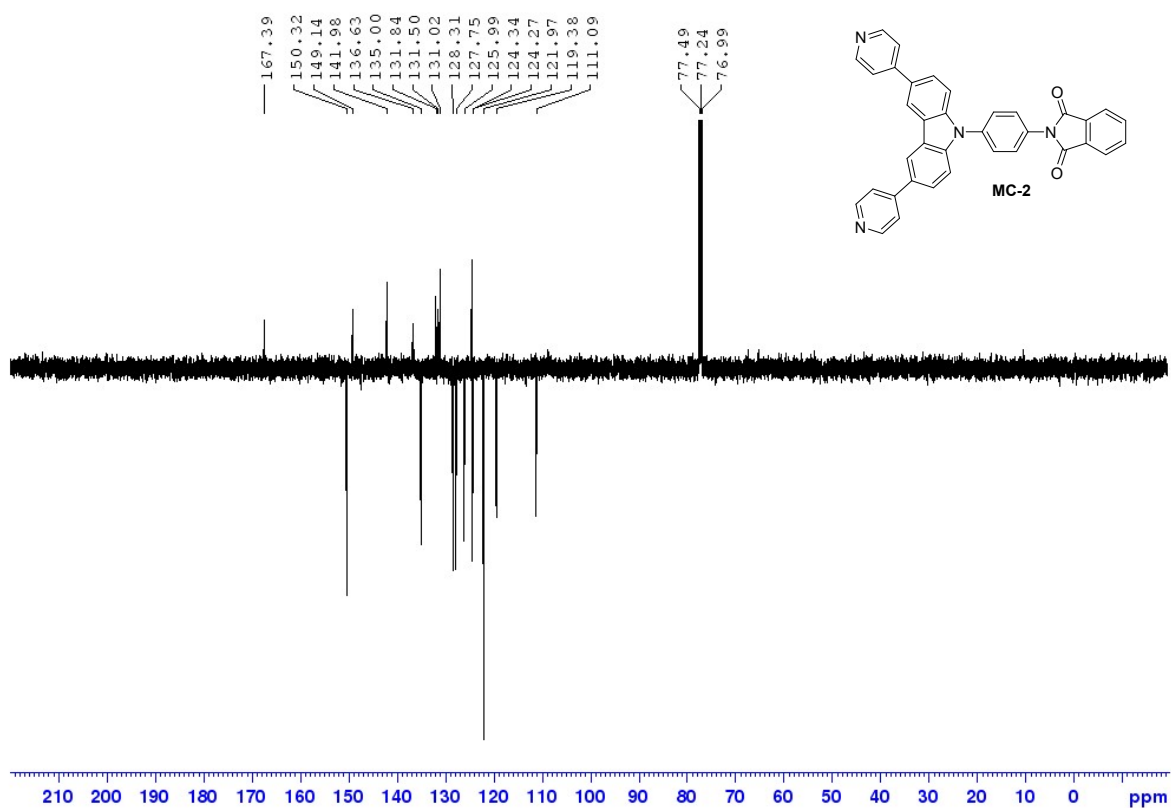


Fig. S14. ¹³C APT NMR (125 MHz, CDCl₃) compound MC-2.

X-ray single crystal analysis

The X-ray data for colorless crystal of **1** were obtained at 150K using Oxford Cryostream low-temperature device with a Bruker D8-Venture diffractometer equipped with Mo (Mo/K_{α} radiation; $\lambda = 0.71073 \text{ \AA}$) microfocus X-ray ($1\mu\text{S}$) source, Photon CMOS detector and Oxford Cryosystems cooling device was used for data collection. Obtained data were treated by XT-version 2014/5 and SHELXL-2017/1 software implemented in APEX3 v2016.9-0 (Bruker AXS) system. [3] $R_{\text{int}} = \sum |F_o^2 - F_{o,\text{mean}}^2| / \sum F_o^2$, $S = [\sum(w(F_o^2 - F_c^2)^2) / (N_{\text{diffrs}} - N_{\text{params}})]^{1/2}$ for all data, $R(F) = \sum ||F_o| - |F_c|| / \sum |F_o|$ for observed data, $wR(F^2) = [\sum(w(F_o^2 - F_c^2)^2) / (\sum w(F_o^2)^2)]^{1/2}$ for all data. Crystallographic data for structural analysis has been deposited with the Cambridge Crystallographic Data Centre, CCDC no. 2206624. Copies of this information may be obtained free of charge from The Director, CCDC, 12 Union Road, Cambridge CB2 1EY, UK (fax: +44-1223-336033; e-mail: deposit@ccdc.cam.ac.uk or www: <http://www.ccdc.cam.ac.uk>).

The frames for the compound were integrated with the Bruker SAINT software package using a narrow-frame algorithm. Data were corrected for absorption effects using the Multi-Scan method (SADABS). The structures were solved and refined using the Bruker SHELXTL Software Package. Hydrogen atoms were mostly localized on a difference Fourier map, however to ensure uniformity of treatment of crystal, most of the hydrogen atoms were recalculated into idealized positions (riding model) and assigned temperature factors $H_{\text{iso}}(\text{H}) = 1.2 U_{\text{eq}}$ (pivot atom). H atoms in aromatic rings were placed with C-H distances of 0.93 \AA . N-H bonds were fixed to 0.88 \AA .

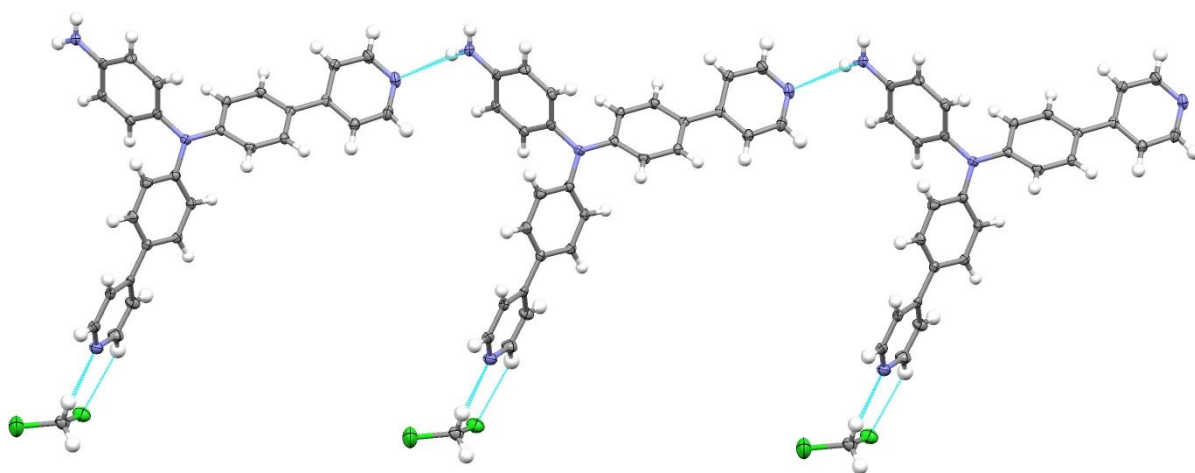


Fig. S15. H-bond architecture in **1**.

Table S1: Experimental details for structure determination of **1**.

Crystal data	
Chemical formula	C ₂₉ H ₂₄ Cl ₂ N ₄
M_r	499.42
Crystal system, space group	Monoclinic, $P2_1/c$
Temperature (K)	150
a, b, c (Å)	16.9736 (7), 14.8656 (5), 19.4029 (7)
β (°)	95.025 (1)
V (Å ³)	4877.0 (3)
Z	8
Radiation type	Mo $K\alpha$
μ (mm ⁻¹)	0.29
Crystal size (mm)	0.26 × 0.13 × 0.08
Data collection	
Diffractionmeter	Bruker D8 - Venture
Absorption correction	Multi-scan <i>SADABS2016/2</i> - Bruker AXS area detector scaling and absorption correction
T_{\min}, T_{\max}	0.653, 0.746
No. of measured, independent and observed [$I > 2\sigma(I)$] reflections	83727, 9070, 6946
R_{int}	0.092
$(\sin \theta/\lambda)_{\text{max}}$ (Å ⁻¹)	0.606
Refinement	
$R[F^2 > 2\sigma(F^2)], wR(F^2), S$	0.057, 0.122, 1.07
No. of reflections	9070
No. of parameters	631
No. of restraints	528
H-atom treatment	H-atom parameters constrained
$\Delta\rho_{\text{max}}, \Delta\rho_{\text{min}}$ (e Å ⁻³)	0.41, -0.49

Computer programs: Bruker Instrument Service vV6.2.3, *APEX3* v2018.1-0 (Bruker AXS), *SAINT* V8.38A (Bruker AXS Inc., 2016), *SHELXT* 2014/5 (Sheldrick, 2014), *SHELXL2017/1* (Sheldrick, 2017), Bruker *SHELXTL*.

Table S2: Hydrogen-bond geometry (Å, °) for structure of **1**.

$D-H\cdots A$	$D-H$	$H\cdots A$	$D\cdots A$	$D-H\cdots A$
N4—H4B ⁱ ⋯N2 ⁱ	0.88	2.33	3.049 (3)	139
N8—H8A ⁱ ⋯N6 ⁱⁱ	0.88	2.30	2.998 (3)	136

Symmetry codes: (i) $x, y-1, z$; (ii) $x, y+1, z$.

Spatial arrangement of carbazole derivative 2

Visualization of the almost perpendicular position of phenyl ring relative to the carbazole unit with a torsion angle 91.58° . Structures were optimized using Gaussian 16W at the B3LYP/6-311++G(2d,p) level and visualized with Mercury[4].

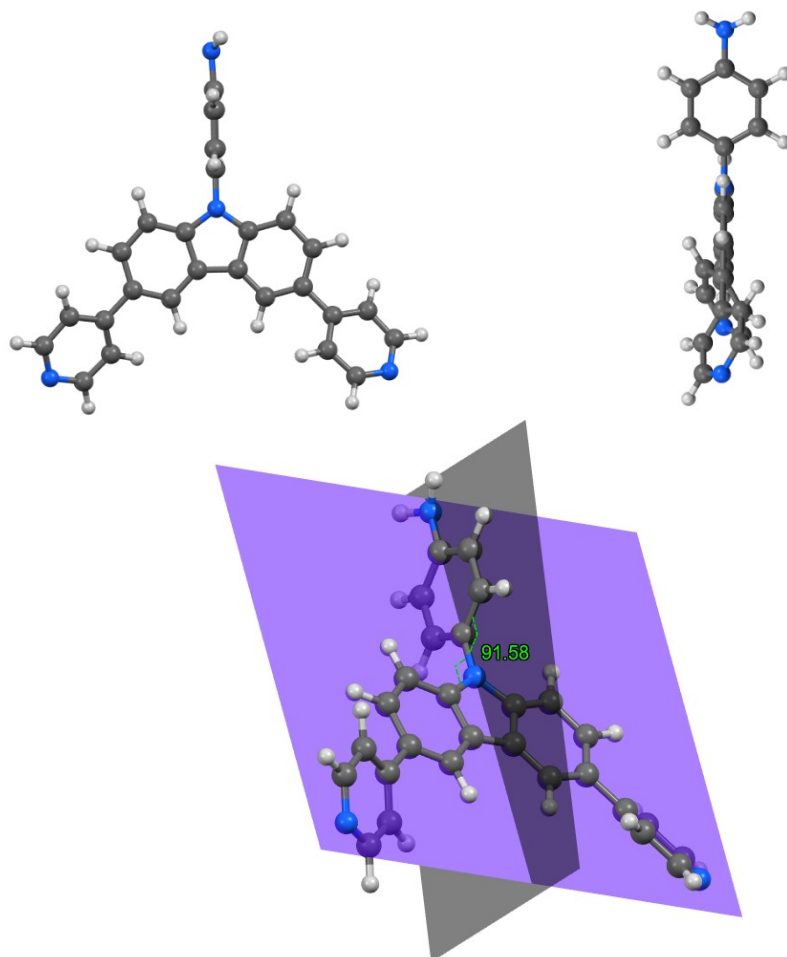


Fig. S16. Spatial arrangement of **2** with a torsion angle visualization (in degrees) amongst phenyl and carbazole unit.

Electrochemical properties

The electrochemical behavior of target molecules was investigated by cyclic voltammetry in THF containing 0.1 M Bu_4NPF_6 in a three electrode cell by cyclic voltammetry (CV). The working electrode was glassy carbon disk (1 mm in diameter). Leak-less Ag/AgCl electrode (SSCE) containing filling electrolyte (3.4 M KCl) and titanium rod with a thick coating of platinum were used as the reference and auxiliary electrodes. All peak potentials are given vs. SSCE. Abbreviations of used electrodes are as following: SSCE – silver/silver chloride electrode; SCE – saturated calomel electrode; SHE – standard hydrogen electrode.

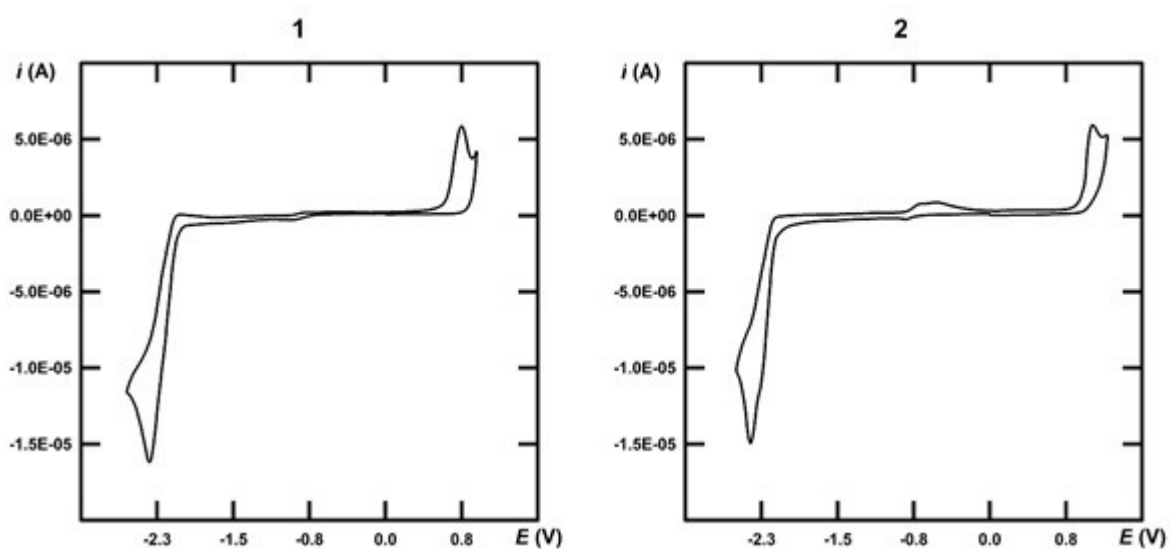


Fig. S17. Cyclic voltammograms of molecules **1** and **2** measured in THF containing 0.1 M Bu_4NPF_6 at glassy carbon electrode; $\nu = 100 \text{ mVs}^{-1}$.

Thermal properties of comonomers

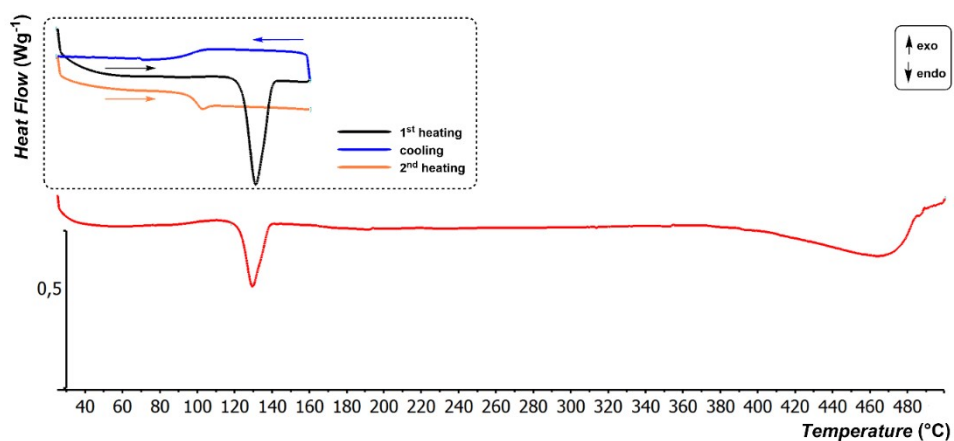


Fig. S18. DSC curves of target molecule **1** determined with a scan rate of 3 °C/min within the range 25–500 °C. Inset: a cooling and re-heating cycle for the first observed endothermic process.

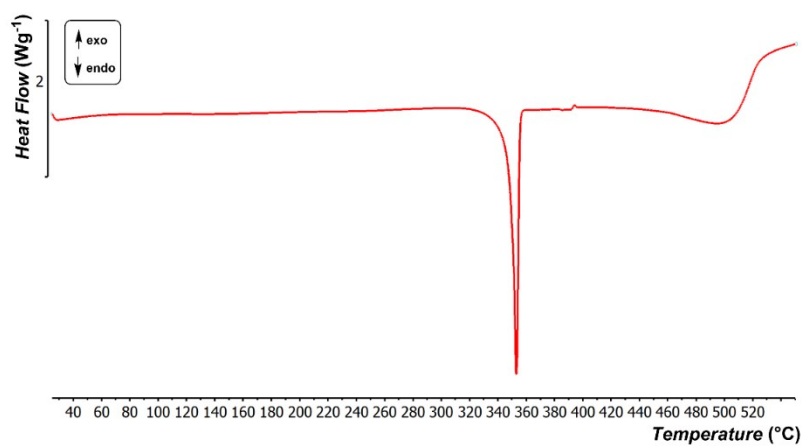


Fig. S19. DSC curve of target molecule **2** determined with a scan rate of 3 °C/min within the range 25–550 °C.

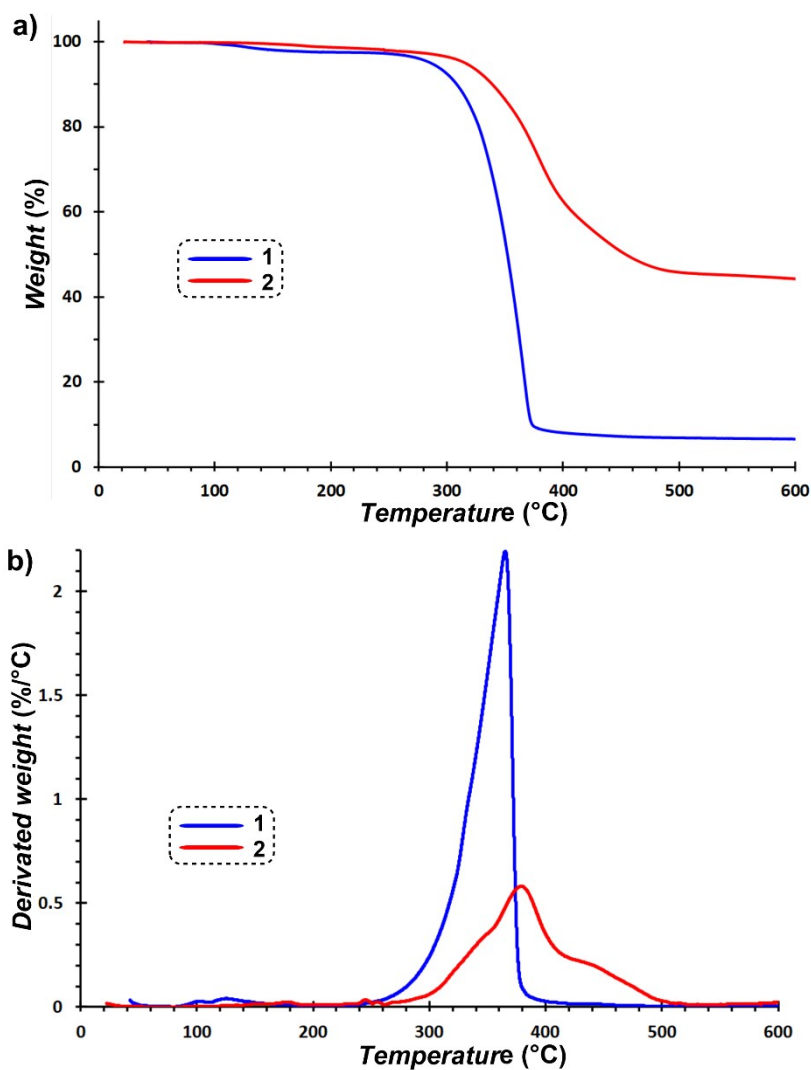


Fig. S20. a) TGA curves of target molecules 1–2 determined with scan rate of 3 °C/min within the range 25–600 °C. b) First derivation of obtained TGA curves for molecules 1–2.

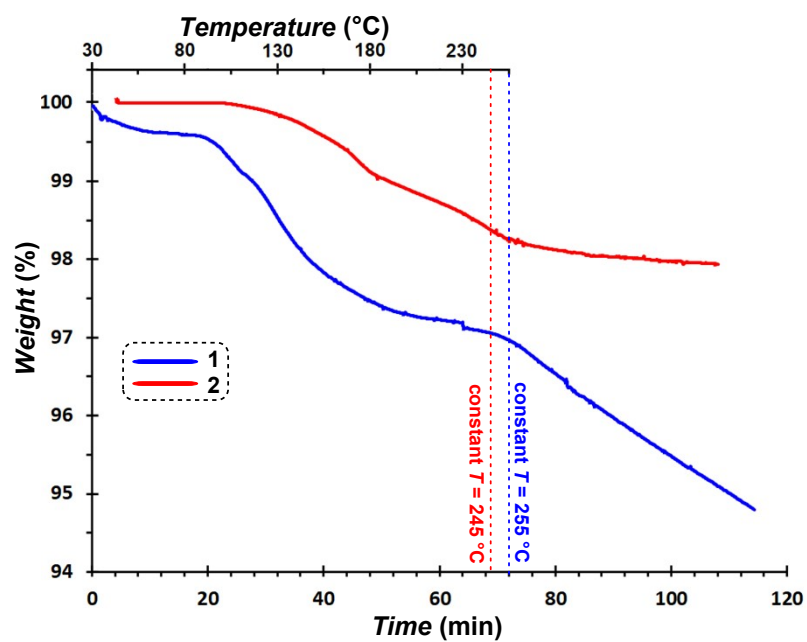


Fig. S21. TGA curves of target molecules 1–2 containing isothermal parts above 245 (2) or 255 °C (1).

Comparison of calculated and experimental UV/Vis absorption spectra

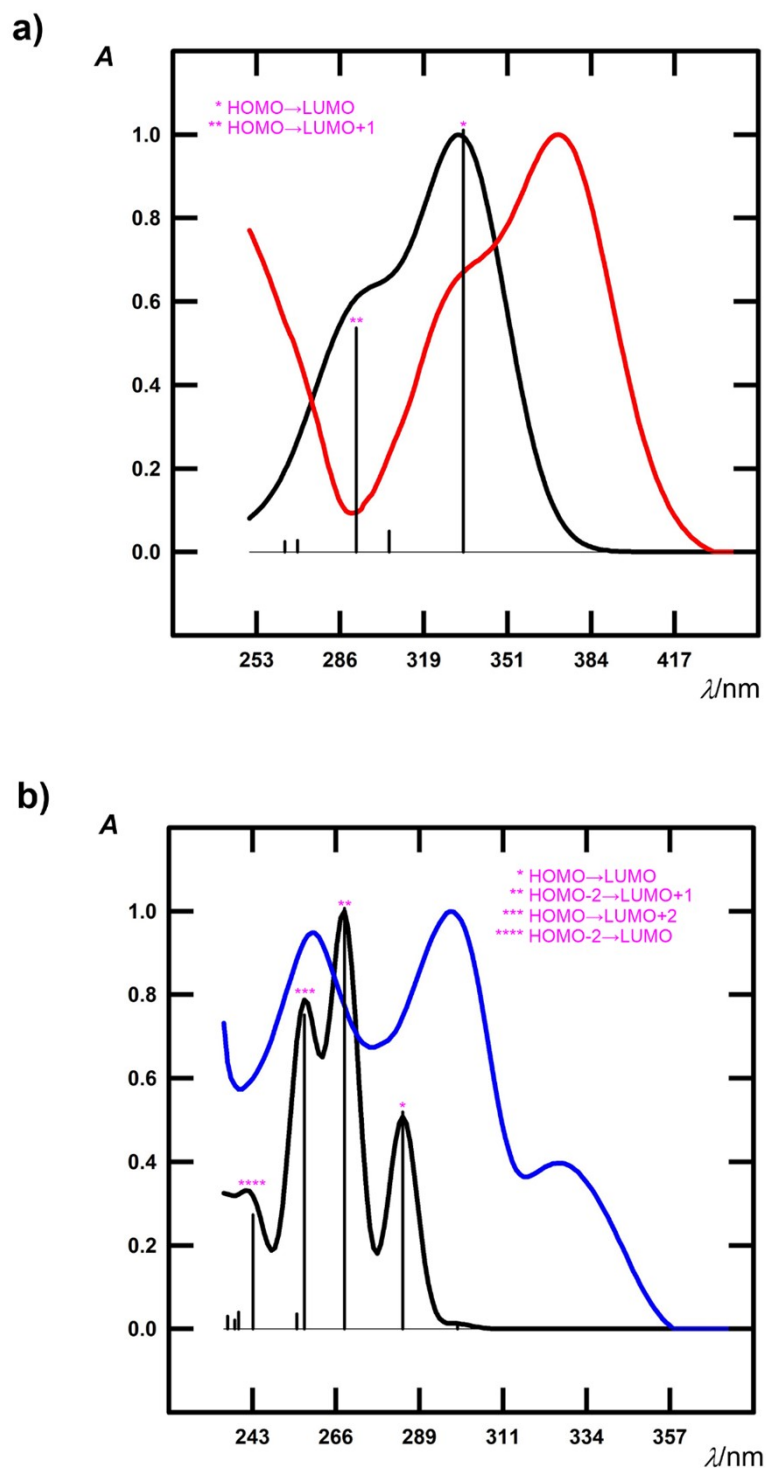


Figure S22. TD-DFT (nstates = 10) CAM-B3LYP/6-311++G(2d,p) calculated (black) UV-Vis spectra of chromophores a) **1** and b) **2** in THF. Black vertical lines represent oscillator strengths (f). The colour curves are experimentally obtained UV-Vis spectra in THF. Both spectra were overlapped and normalized to have maximal absorbance (A) of 1 using OPchem software[5].

Visualization of frontier molecular orbitals

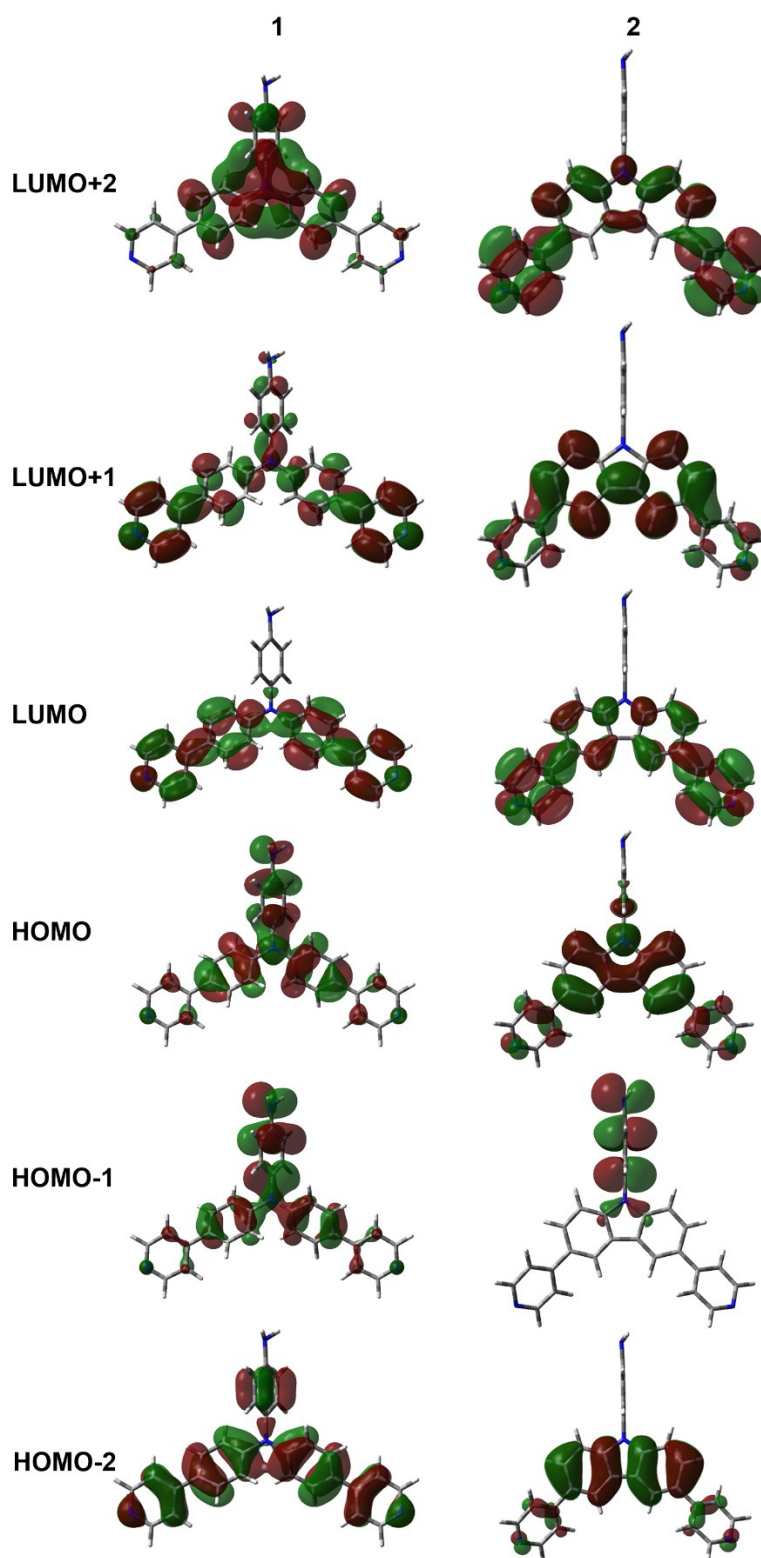


Figure S23. Frontier orbitals of chromophores **1** and **2** were obtained/visualized from DFT calculations performed by using Gaussian 16W at the B3LYP/6-311++G(2d,p) level in THF.

Synthesis of PIs

Synthesis of PI blanks

Two types of PIs, starting from 1,2,4,5-cyclohexanetetracarboxylic dianhydride/2,2-bis[4-(4-aminophenoxy)phenyl]propane (CHDA-BAPP) and 4,4'-(hexafluoroisopropylidene)diphthalic anhydride/2,2'-bis(trifluoromethyl)benzidine (6FDA-TFMB), were investigated. Two undoped and nonemissive PI blanks were synthesized using similar procedure.

To illustrate the general synthetic route towards PI blanks, we describe herein the synthesis of polyimide CHDA-BAPP. Diamine BAPP (821 mg; 2 mmol) and dianhydride CHDA (448 mg; 2 mmol) were dissolved in dimethylacetamide (DMAc) (5.4 ml). The reaction mixture was stirred for 24 h at 25 °C under an inert atmosphere of nitrogen. The resulting polyamic acid (PAA) solution was casted on a clean glass plate as a PAA film. The PAA film was imidized into PI in a high temperature furnace according to the following protocol: (1) heating to 150 °C at a rate of 2 °C/min and annealing at 150 °C for 1 h to remove any residual solvent, (2) heating at a rate of 2 °C/min and annealing at 250 °C for 1 h, (3) heating at a rate of 2 °C/min and annealing at 300 °C for 2 h to complete the imidization process. The imidization process was carried out under high vacuum. After cooling to room temperature, the plate was soaked in warm water for a few minutes and the polyimide film was peeled off automatically. Polyimide (6FDA-TFMB) was synthesized in the same manner using diamine 6FDA (888 mg; 2 mmol) and dianhydride TFMB (640 mg; 2 mmol).

Synthesis of emissive PI films

Twelve end-capped emissive PIs using different ratios (5, 1 and 0.1 mol %) of amines **1** or **2** and diamines BAPP or TFMB and dianhydrides CHDA or 6FDA were prepared. Thickness of the PI films range from 45 – 55 μm. These materials were synthesized using similar procedure as described below for a representative example.

For the synthesis of end-capped emissive polyimides, appropriate molar quantity of diamines was replaced with amines **1** or **2**. The following synthesis of polyimide containing 5 mol. % of **2** is used as an illustrative example. Diamine BAPP (779 mg; 1.9 mmol), dianhydride CHDA (448 mg; 2 mmol) and chromophore **2** (41.2 mg, 0.1 mmol) were dissolved in DMAc (5.4 ml). The reaction mixture was stirred for 24 h at 25 °C under an inert atmosphere of nitrogen. The resulting polyamic acid (PAA) solution was casted on a clean glass plate as a PAA film. The PAA film was imidized into PI (polyimide) in a high temperature furnace according to the following protocol: (1) heating to 150 °C at a rate of 2 °C/min and annealing at 150 °C for 1 h to remove any residual solvent, (2) heating at a rate of 2 °C/min and annealing at 250 °C for 1 h, (3) heating at a rate of 2 °C/min and annealing at 300 °C for 2 h to complete the imidization process. The imidization process was carried out under high vacuum. After cooling to room temperature, the plate was soaked in warm water for a few minutes and the polyimide film was peeled off automatically.

FTIR spectroscopy

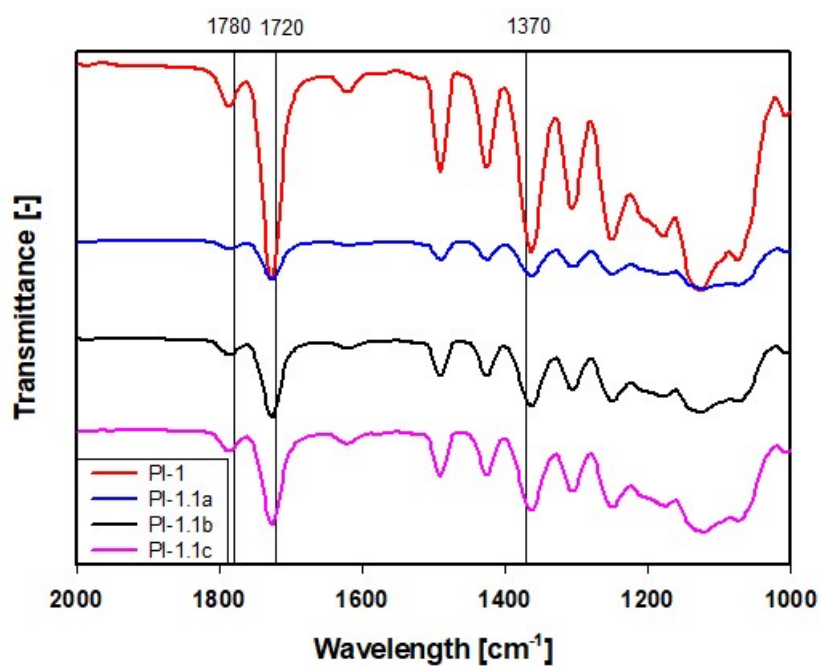


Fig. S24. HATR-FTIR spectra of PI-1 and PI1.1a-c.

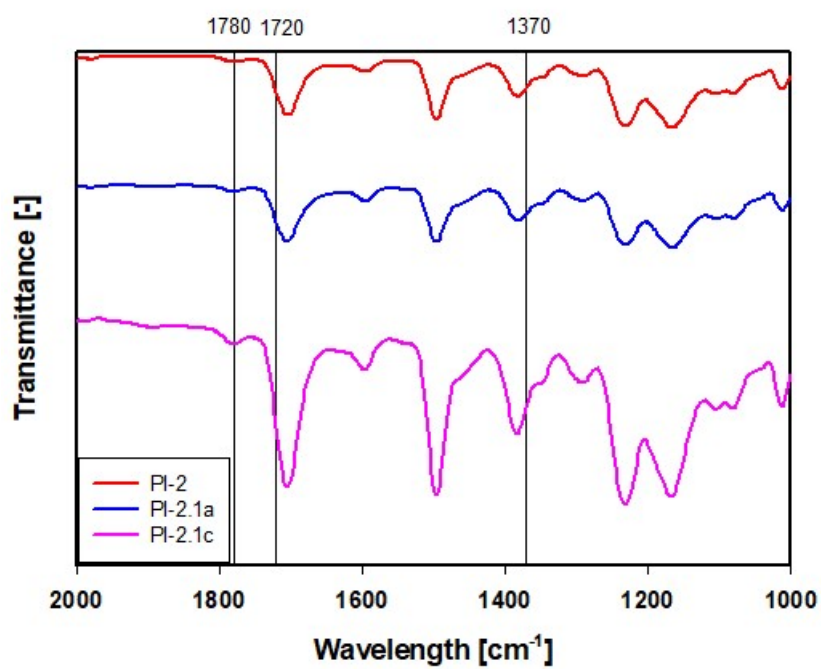


Fig. S25. HATR-FTIR spectra of PI-2, PI2.1a and PI2.1c.

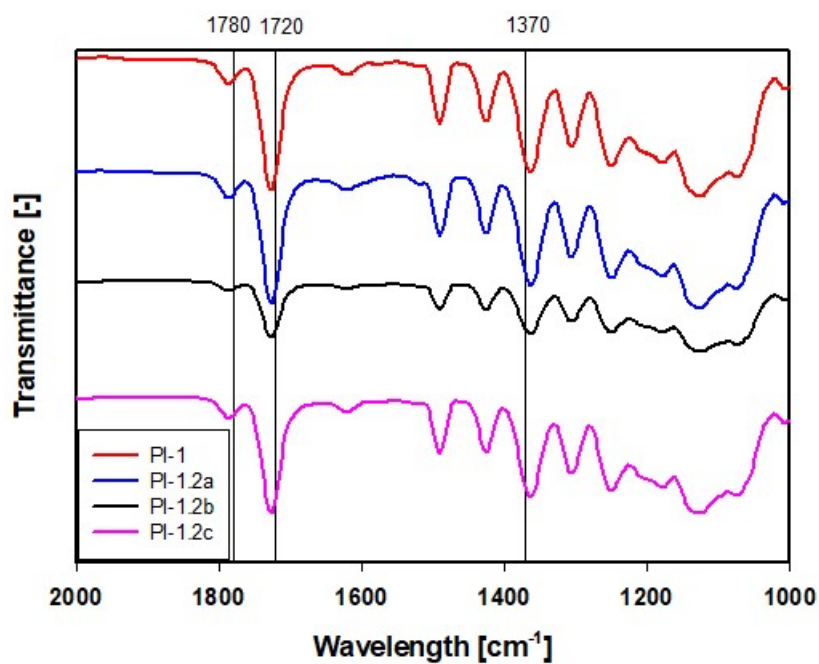


Fig. S26. HATR-FTIR spectra of PI-1 and PI1.2a-c.

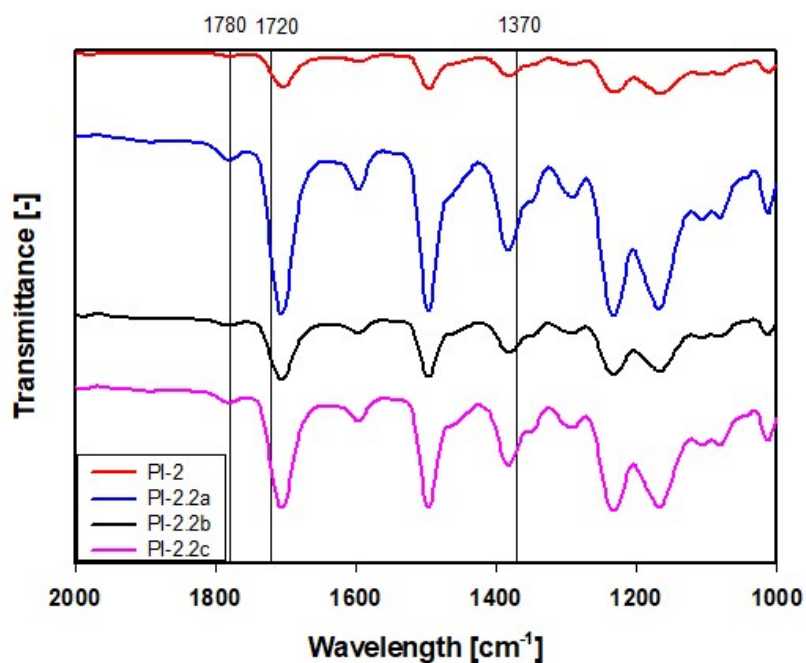


Fig. S27. HATR-FTIR spectra of PI-2 and PI2.2a-c.

Photophysical properties of model compounds:

The optical characteristics of model phthalic imides **MC-1** and **MC-2** were investigated in DCM and THF, the measured data are summarized in Table S3 and Fig. S28. The absorption maxima of carbazole **MC-2** and TPA **MC-1** were found within the UV area at 299 nm and ~345 nm respectively in both DCM and THF (Fig. S28a, S28b). When compared to original **1** and **2**, the absorption maxima of **MC-1/2** are blue shifted by ca 25nm, which reflects diminished donating ability upon attaching two carbonyl moieties.

Model compounds **MC-1** and **MC-2** are weakly emissive in DCM and THF (Fig. S28c, S28d), with the emission maxima within the range of 381 to 442 nm. According to the hypsochromically shifted absorption maxima, their emission maxima are blue shifted by 110/50 nm.

Table S3. Photophysical properties of chromophores **MC-1/2**.

Compd	Solvent	λ_{max}^A [nm (eV)]	ϵ [10 ³ M ⁻¹ cm ⁻¹]	λ_{max}^E [nm]	Stokes shift [cm ⁻¹]
MC-1	DCM	346 (3.58)	36.0	442	6277
	THF	344 (3.60)	44.3	424	5485
MC-2	DCM	299 (4.15)	44.7	383	7335
	THF	299 (4.15)	45.0	381	7198

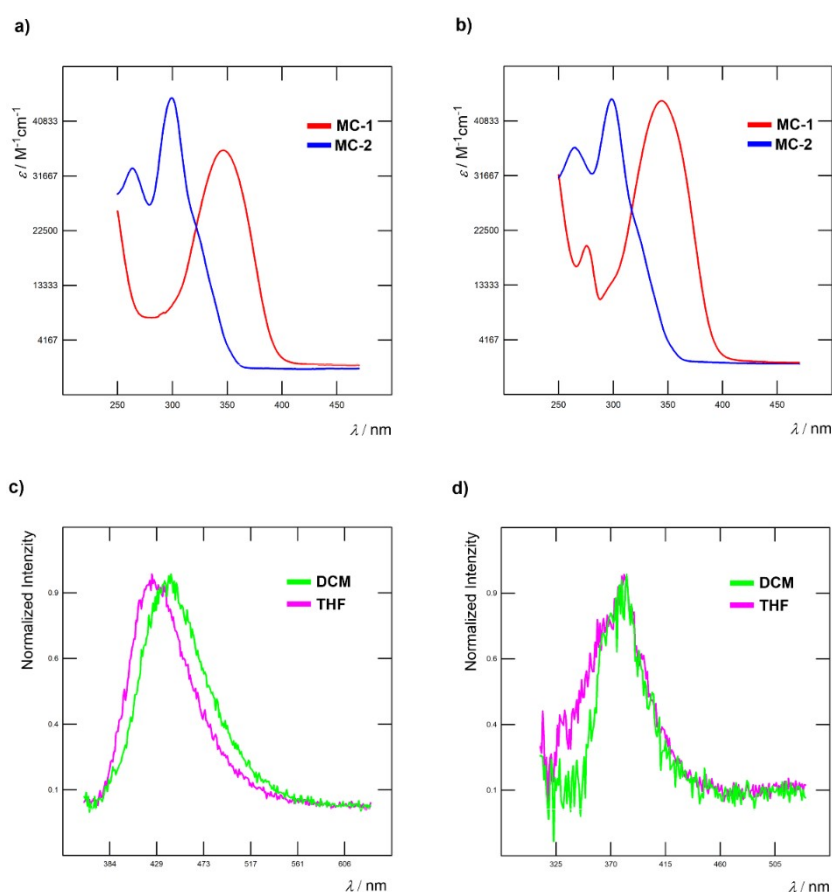


Fig. S28. Absorption spectra of **MC-1** and **MC-2** in a) DCM and b) THF. Normalized emission spectra of chromophores in DCM and THF solutions c) **MC-1** d) **MC-2**.

Table S4. Photographs of PI films.

PI film	Ambient light	UV (254 nm)	UV (365 nm)
PI-1.1a			
PI-1.1b			
PI-1.1c			
PI-2.1a			
PI-2.1c			
PI-1.2a			
PI-1.2b			
PI-1.2c			
PI-2.2a			
PI-2.2b			
PI-2.2c			

CIE chromaticity diagrams of PI films

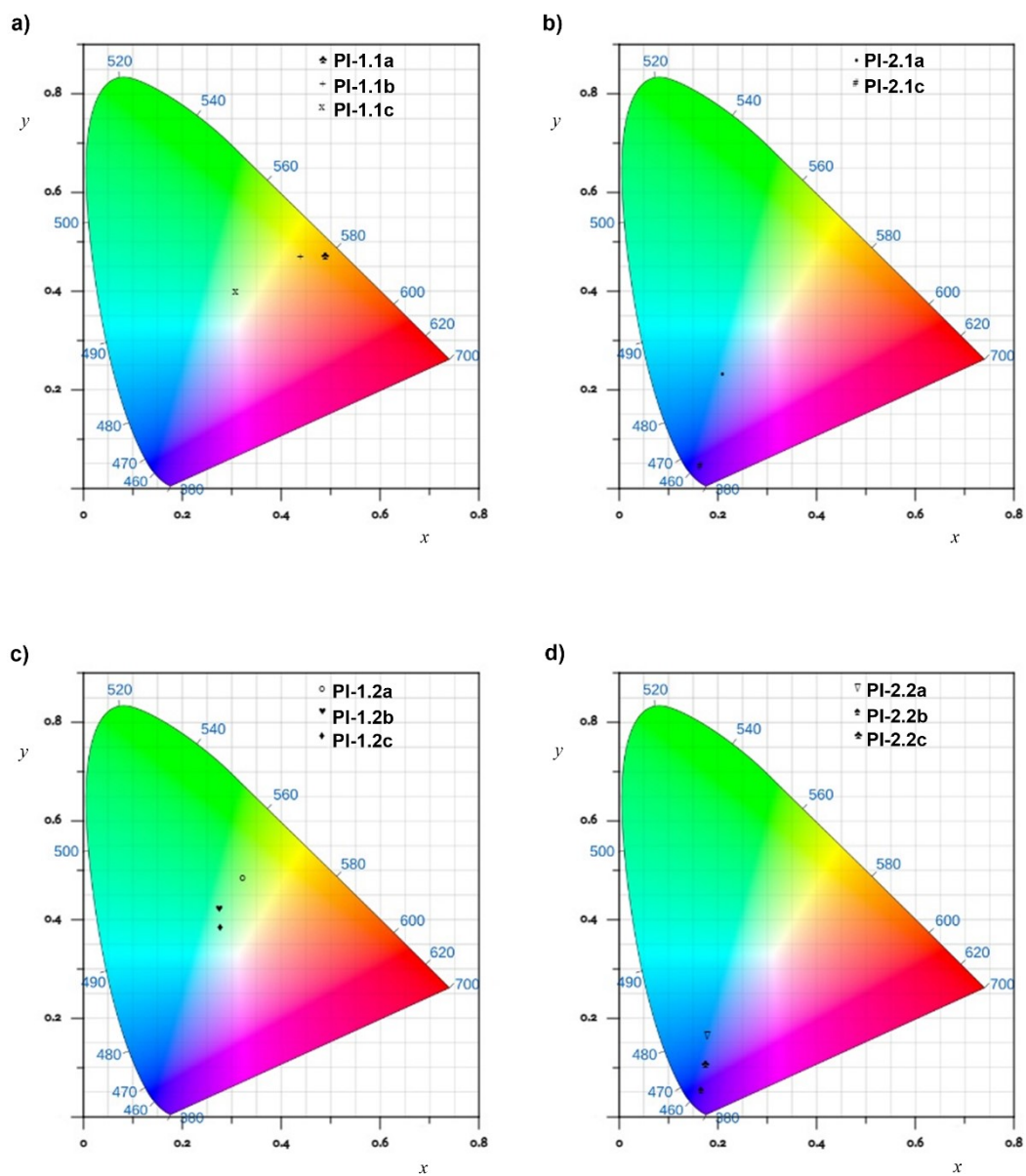


Figure S29. CIE chromaticity diagram 1931 of emissive PI film series a) **PI1.1a-c**, b) **PI2.1a** and c, c) **PI1.2a-c**, d) **PI2.2a-c**. [6]

Thermal properties of PI films

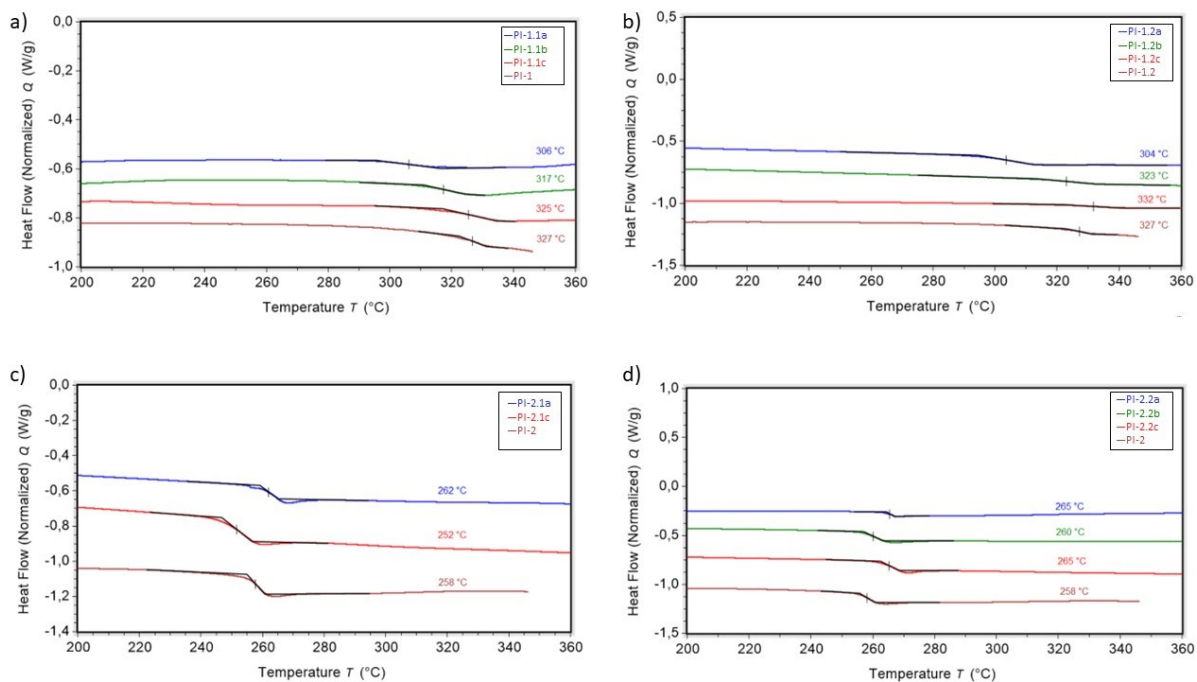


Fig. S30. DSC curves of PI films.

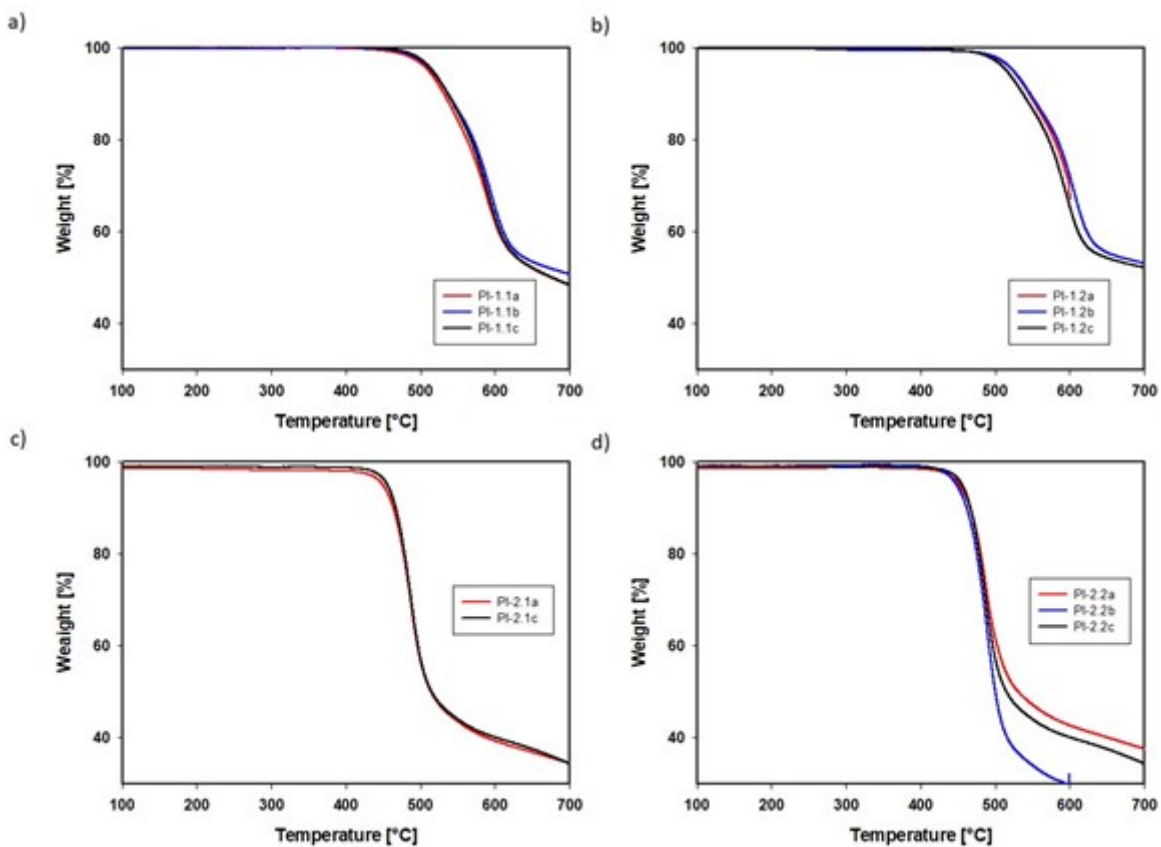


Fig. S31. TGA curves of PI films.

References:

- [1] E. Ishow, A. Brosseau, G. Clavier, K. Nakatani, R.B. Pansu, J. Vachon, P. Tauc, D. Chauvat, C.R. Mendonça and E. Piovesan, *J. Am. Chem. Soc.*, 2007, **129**, 8970–8971.
- [2] K. Tahara, T. Nakakita, S. Katao and J.I. Kikuchi, *Chem. Commun.*, 2014, **50**, 15071–15074.
- [3] G.M. Sheldrick, SHELXT - Integrated space-group and crystal-structure determination, *Acta Crystallogr. Sect. A Found. Crystallogr.* 71 (2015) 3–8.
- [4] C.F. Macrae, I. Sovago, S.J. Cottrell, P.T.A. Galek, P. McCabe, E. Pidcock, M. Platings, G.P. Shields, J.S. Stevens, M. Towler, P.A. Wood, Mercury 4.0 : from visualization to analysis, design and prediction, *J. Appl. Crystallogr.* 53 (2020) 226–235.
- [5] Pytela O. OPChem., (n.d.). <http://bures.upce.cz/OPgm>
- [6] E.H.H. Hasabeldaim, CIE chromaticity diagram 1931, (2021). <https://sciapps.scisim.com/CIE1931.html>.